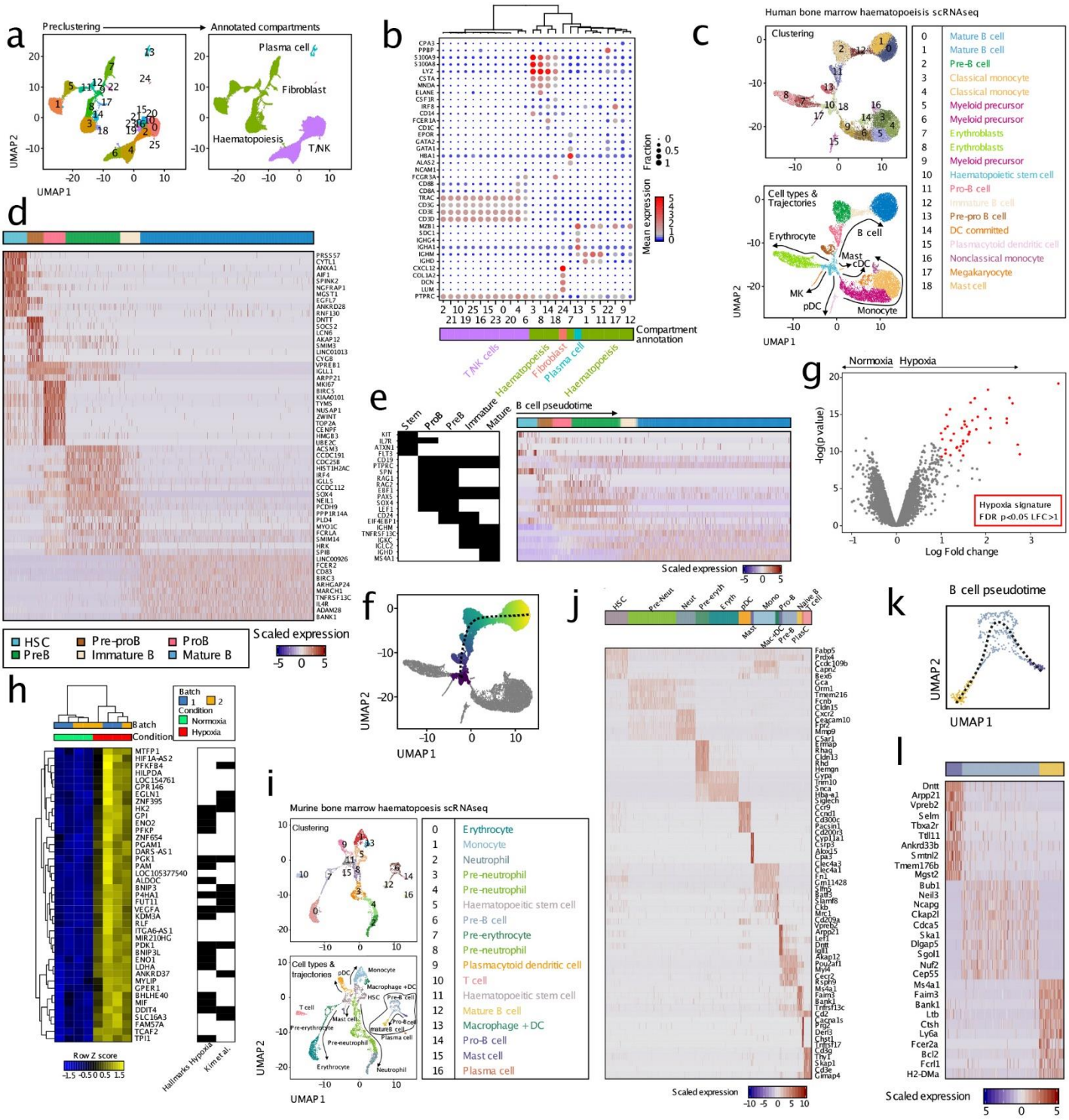

Supplementary Figure 1

Single cell analysis of human bone marrow (BM; Human Cell Atlas dataset) and murine BM (Tabula Muris dataset) used to generate cellular differentiation trajectories and scaled hypoxia geneset scores, against B cell developmental pseudotime

Analysis of human BM:

(a) Initial pre-clustering solution used to generate broad compartments. Left; PAGA-initialized UMAP plot colored and labelled by Leiden cluster. Right; PAGA-initialized UMAP plot colored by annotated compartment.

(b) Heatmap showing average expression and fractional expression per cluster of key canonical genes, supporting annotation of clusters shown in (a) to broad compartments. Clusters annotated as “hematopoiesis” (green), are retained for downstream analysis.

(c) Top; PAGA-initialized UMAP plot colored and labelled according to Leiden clusters after reanalysis of the “hematopoiesis” compartment. Bottom; PAGA-initialized UMAP plot colored and labelled according to annotated cell type and annotated according to differentiation trajectory; Right; table showing annotation of each Leiden cluster to cell type or differentiation state.

Supplementary Figure 1

(d) Heatmap showing scaled expression values of the top 10 unique marker genes for each annotated cell state involved in B cell differentiation.
(e) Left; expression of canonical genes involved in B cell development derived from the literature; Right; scaled expression of these genes ordered by B cell pseudotime.
(f) PAGA-initialized UMAP plot colored by B cell pseudotime, cells not participating in this trajectory are de-colored. Principal curve (calculated using *Slingshot*) is overlaid.
(g) Microarray analysis of purified human peripheral blood B cells cultured in normoxia or hypoxia (1% O_2) for 24 h, pooled from two independent experiments, n=4 biologically independent primary cell cultures. Depicted; Volcano plot showing differential expression (Linear models for microarray analysis (Limma)) between hypoxia and normoxia. Genes with a log fold change >1 and Benjamini-Hochberg False Discovery Rate (FDR) adjusted $P< 0.05$ are colored red and were used as the hypoxia geneset in Fig. 1a. *P*-values were calculated from moderated two-sided t-statistics. For Tabula Muris BM B cells, genesets used are murine orthologues of the human geneset.
(h) Heatmap of row normalized expression scores of differentially expressed genes identified in (g). Right; overlap with other hypoxia genesets (MSigDB Hallmarks hypoxia and Kim *et al*. 2006). Genes present in both the experimental hypoxia geneset generated in (g) and the reference genesets are colored in black and show that this bespoke geneset has a mixture of genes that overlap with common hypoxia genes and those specific to human B cells.

Analysis of murine BM:
(i) Top; PAGA-initialized UMAP plot colored and labelled by Leiden cluster. Bottom; PAGA-initialized UMAP plot colored and labelled by annotated cell type or differentiation state. The plot is annotated according to differentiation trajectory. Right; table showing annotation of each Leiden cluster.
(j) Heatmap showing scaled expression values of the top 5 unique marker genes for each annotation in (i).
(k) PAGA-initialized UMAP using the initial embedding coordinates showing only B cell development. Principal curve (calculated using *Slingshot*) is overlaid.
(l) Heatmap showing scaled expression values of the top 10 unique marker genes for each B cell development state.

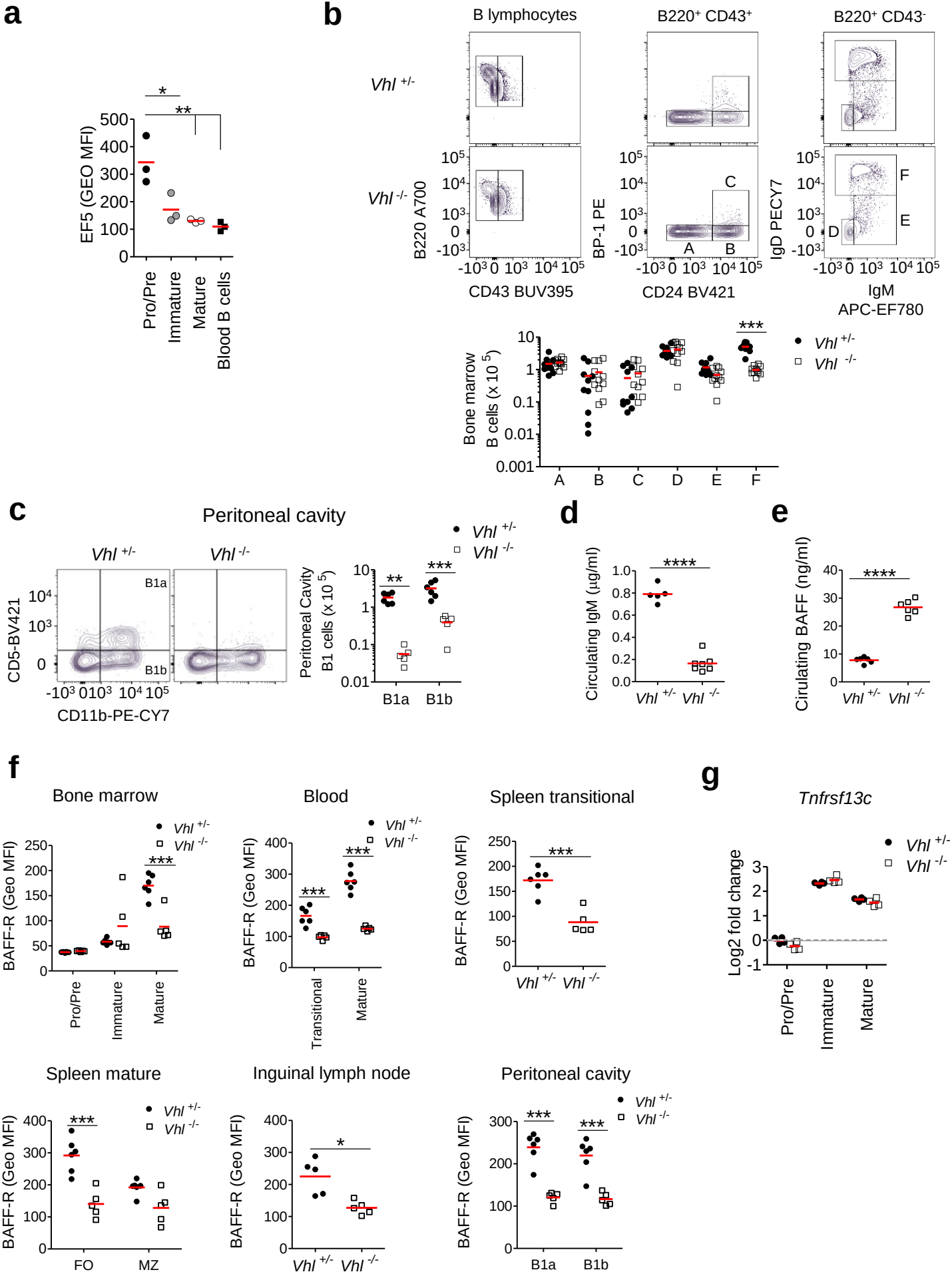

Supplementary Figure 2

***Vhl* deletion in B cells leads to peripheral B cell lymphopenia and associated clinical characteristics (low circulating IgM, high circulating BAFF and low BAFF-receptor (BAFF-R) expression). Splenic T cells were reduced**

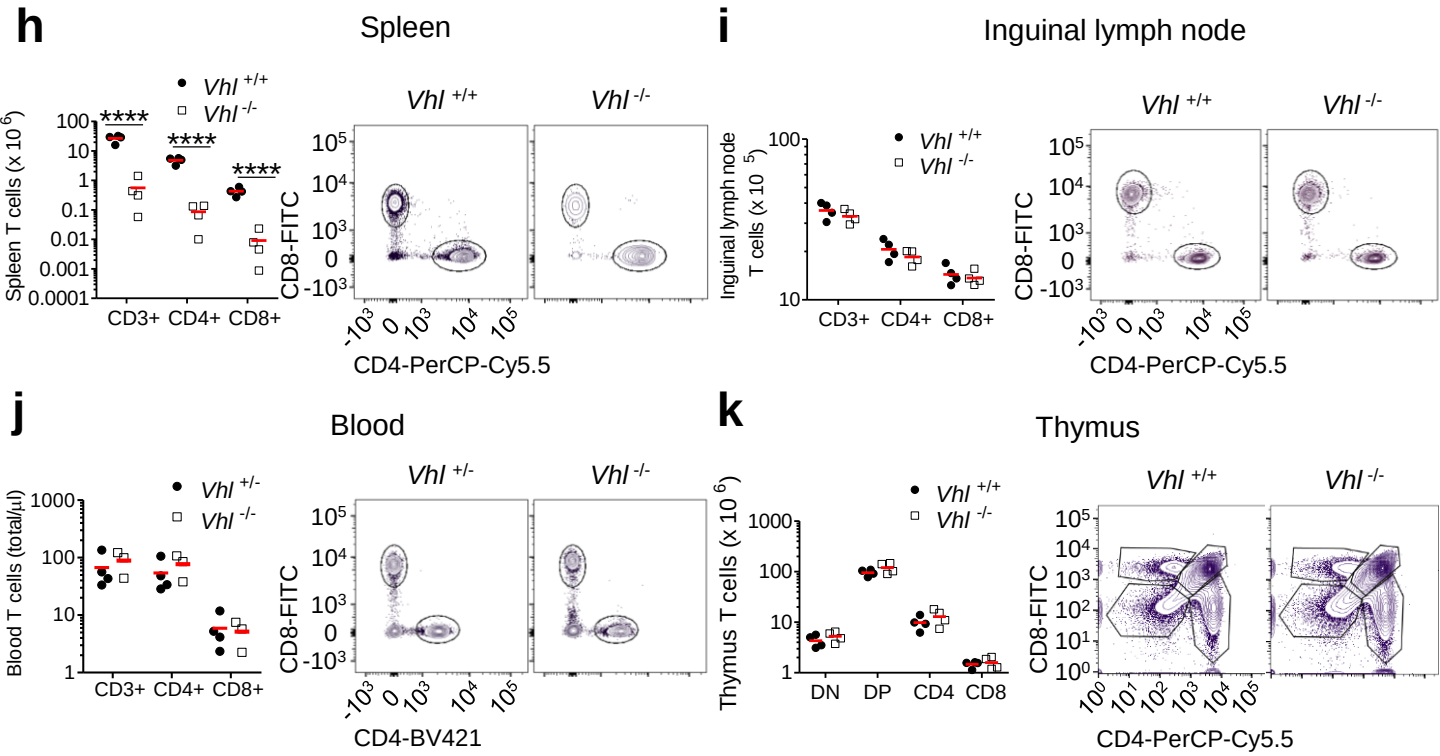

Supplementary Figure 2

(a) Comparison of EF5 levels in B cells from BM and left ventricular blood. Displayed, quantified EF5 levels (Geo MFI) detected by anti-EF5 staining in BM B cells (gated as in Figure 1b) and blood transitional B cells ($B220^+IgM^+IgD^-$). *P<0.05,**P<0.01 one-way ANOVA Tukey post-test. n=3 biologically independent C57BL/6J mice from one experiment.

(b) Flow cytometry showing the gating and absolute numbers of BM B cells (Hardy Fractions A-F) from *Vhl*$^{+/-}$*Mb1-cre* and *Vhl*$^{-/-}$*Mb1-cre* mice. Gated on pre-pro-B (FrA:$B220^+CD43^+CD24^{-/low}BP\text{-}1^-$), Pro-B (FrB: $B220^+CD43^+CD24^+BP\text{-}1^-$), Late pro-B/Early pre-B (FrC: $B220^+CD43^{+/low}CD24^+BP\text{-}1^+$), Late pre-B (FrD: $B220^+CD43^-IgM^-IgD^-$), immature (FrE: $B220^+CD43^-IgM^+IgD^-$), mature (FrF: $B220^+CD43^-IgM^+IgD^+$). ***P<0.001 two-way ANOVA Bonferroni post-test. Data are pooled from three experiments. n=10 *Vhl*$^{+/-}$*Mb1-cre* and 11*Vhl*$^{-/-}$*Mb1-cre* biologically independent mice. Results were confirmed in a further five independent experiments.

(c) Flow cytometry showing the gating and absolute numbers of B1 cells from *Vhl*$^{+/-}$*Mb1-cre* and *Vhl*$^{-/-}$*Mb1-cre* mice in the peritoneal cavity, gated on B1 cells: $CD19^+IgM^+$, B1a: $CD5^+CD11b^+$, B1b: $CD5^-CD11b^+$. **P<0.01, ***P<0.001 two-way ANOVA Bonferroni post-test. n=6 *Vhl*$^{+/-}$*Mb1-cre* and 5 *Vhl*$^{-/-}$*Mb1-cre* biologically independent mice. Data are representative of five independent experiments.

(d) Circulating levels of IgM in *Vhl*$^{+/-}$*Mb1-cre* and *Vhl*$^{-/-}$*Mb1-cre* mice, detected by ELISA. ****P<0.0001 unpaired two-sided t test. n=5 *Vhl*$^{+/-}$*Mb1-cre* and 7 *Vhl*$^{-/-}$*Mb1-cre* biologically independent mice. Data are representative of three independent experiments.

(e) Circulating levels of BAFF in *Vhl*$^{+/-}$*Mb1-cre* and *Vhl*$^{-/-}$*Mb1-cre* mice, detected by ELISA. ****P<0.0001 unpaired two-sided t test. n=6 biologically independent mice per genotype. Data are representative of two independent experiments.

(f) Mean BAFF-R expression (Geo MFI), by flow cytometry, in B cells from *Vhl*$^{+/-}$*Mb1-cre* and *Vhl*$^{-/-}$*Mb1-cre* mice. B cells from peripheral blood were gated on transitional ($B220^+CD93^+$) and mature ($B220^+CD93^-$). All other B cells were gated as in Figure 1. ***P<0.001 two-way ANOVA Bonferroni post-test, *P<0.05, ***P<0.001 unpaired two-sided t test. n=5 *Vhl*$^{+/-}$*Mb1-cre* (ILN), 6 *Vhl*$^{+/-}$*Mb1-cre* (BM, blood, spleen, peritoneal cavity) and 5 *Vhl*$^{-/-}$*Mb1-cre* biologically independent mice. Data are representative of three independent experiments.

(g) *Tnfrsf13c* gene expression data from flow-sorted BM B cells (described in Figures 4e-g). Expression of *Tnfrsf13c* that encodes the BAFF-R is similar between *Vhl*$^{+/-}$*Mb1-cre* and *Vhl*$^{-/-}$*Mb1-cre* B cells suggesting that reductions in BAFF-R protein are not at the level of transcriptional regulation by HIF-1. n=4 biologically independent mice per genotype, from one experiment. Data are from GEO: GSE129513.

Flow cytometry showing the gating and absolute numbers of T cells in;

(h) Spleen

(i) ILN

(j) Blood

(k) Thymus. DN = double negative for CD4 and CD8. DP = double positive for CD4 and CD8.

(h-k) Gated on CD4+ ($B220^-CD3^+CD4^+CD8^-$) and CD8+ ($B220^-CD3^+CD4^-CD8^+$) T cells.****P<0.0001 two-way ANOVA Bonferroni post-test. Control mice were *Vhl*$^{+/-}$*Mb1-cre* or *Vhl*$^{+/+}$*Mb1-cre*. **(h,i,k)** n=4 biologically independent mice per genotype, **(j)** n=4 *Vhl*$^{+/-}$*Mb1-cre* and 3 *Vhl*$^{-/-}$*Mb1-cre* biologically independent mice. **(h-j)** Data are representative of three independent experiments.

(a-k) Symbols represent individual mice, bars mean ± S.D.

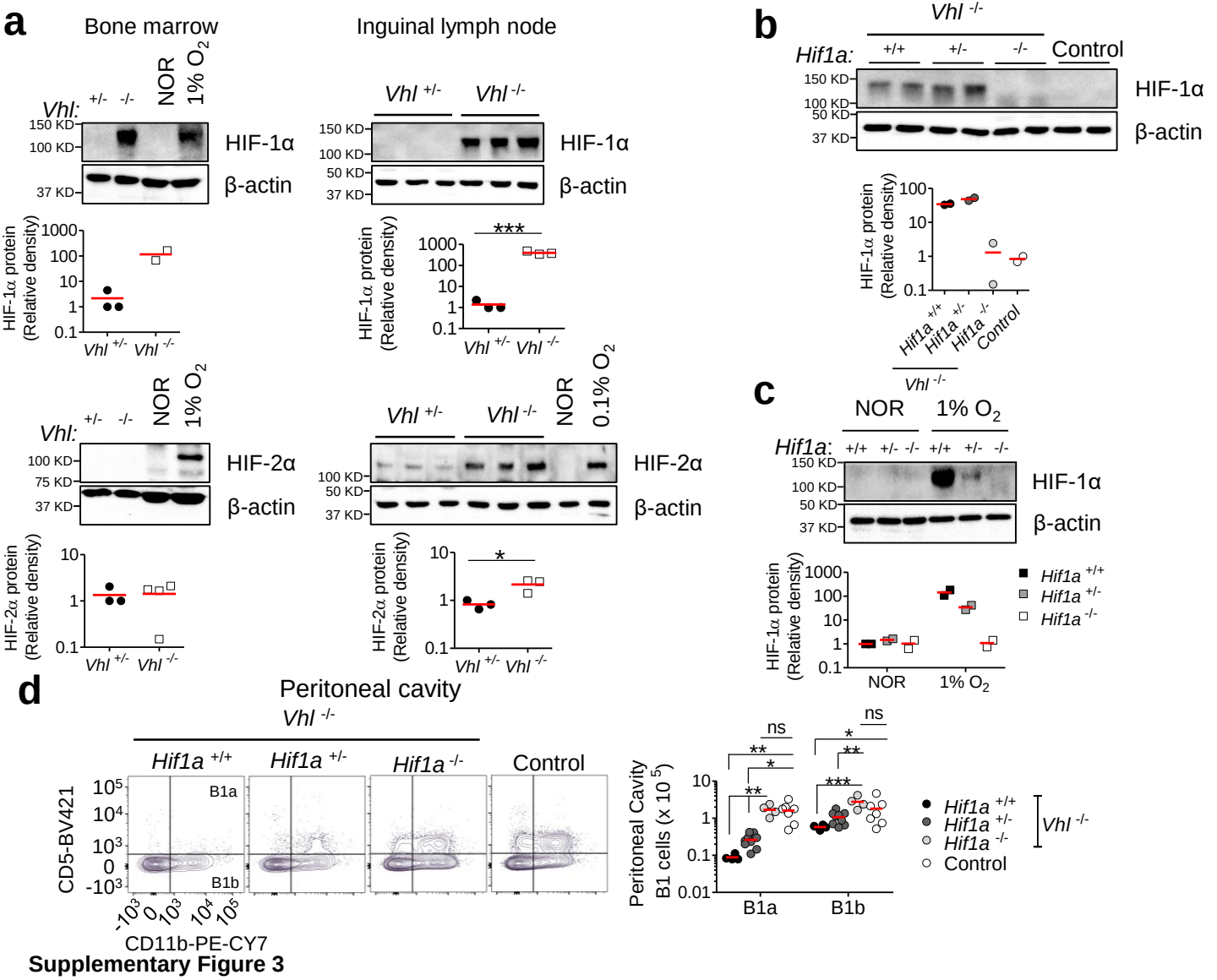

Supplementary Figure 3

HIF-1α and HIF-2α expression in B cells from *Vhl$^{-/-}$Mb1-cre* mice. *Mb1-cre* mice carrying *Hif1a$^{-/-}$* alleles do not express HIF-1α protein when *Vhl* is deleted or when exposed to hypoxia. B1 cell loss is HIF-1α dependant

(a) Immunoblots of HIF-1α and HIF-2α protein in BM B cells isolated by B220 positive selection, and in homogenised ILNs from *Vhl$^{+/-}$Mb1-cre* and *Vhl$^{-/-}$Mb1-cre* mice. Splenocytes cultured for 18 h under normoxia (NOR) and 0.1% or 1% O_2 were used as negative and positive controls for HIF-α expression. Quantification of relative protein expression is shown; BM HIF-1α, *n*=3 *Vhl$^{+/-}$Mb1-cre* and 2 *Vhl$^{-/-}$Mb1-cre* and BM HIF-2α, *n*=3 *Vhl$^{+/-}$Mb1-cre* and 4 *Vhl$^{-/-}$Mb1-cre* biologically independent mice, from two independent blots. ILN blots and quantified protein expression, *n*=3 *Vhl$^{+/-}$Mb1-cre* and 3 *Vhl$^{-/-}$Mb1-cre* biologically independent mice; blots are representative of two independent blots. ***P<0.001 unpaired two-sided t test.

(b) Immunoblot and quantification of HIF-1α protein expression in homogenised ILNs from *Vhl$^{-/-}$Mb1-cre* mice carrying alleles for *Hif1a$^{+/+}$*, *Hif1a$^{+/-}$* or *Hif1a$^{-/-}$* and from control mice (*Vhl$^{+/-}$Hif1a$^{+/+}$Mb1-cre), n*=2 biologically independent mice per genotype; data, representative of two independent experiments. HIF-1α expression is ablated in *Vhl$^{-/-}$Mb1-cre* mice carrying *Hif1a$^{-/-}$* alleles.

(c) Immunoblot of HIF-1α expression in negatively-isolated splenic B cells from *Hif1a$^{+/+}$Mb1-cre*, *Hif1a$^{+/-}$Mb1-cre*, *Hif1a$^{-/-}$Mb1-cre* mice. B cells were cultured under normoxia or 1% O_2 for 2 h. Under 1% O_2, HIF-1α is ablated in *Hif1a$^{-/-}$Mb1-cre* B cells and decreased in *Hif1a$^{+/-}$Mb1-cre* versus *Hif1a$^{+/+}$Mb1-cre* B cells. Quantification of relative protein expression is shown (*n*=2 biologically independent mice per genotype, from two independent experiments).

(a-c) β-actin was used as the loading control. Relative protein expression was quantified by densitometric analysis of background adjusted normalised band volumes and calculated as fold change of a reference lane (either a normoxic control or one negative for HIF-α). Therefore lanes negative for HIF-α have a value of 1. Symbols represent individual mice, bars means ± S.D.

(d) Flow cytometry showing the gating and absolute numbers of peritoneal B1 cells from *Vhl$^{-/-}$Mb1-cre* mice carrying *Hif1a$^{+/+}$*, *Hif1a$^{+/-}$* and *Hif1a$^{-/-}$* alleles, and from *Vhl$^{+/-}$Hif1a$^{+/+}$Mb1-cre* control mice, gated as in Supplementary figure 2c. *P<0.05, **P<0.01, ***P<0.001 two-way ANOVA Bonferroni post-test. *n*=4 *Vhl$^{-/-}$Hif1a$^{+/+}$Mb1-cre*, 9 *Vhl$^{-/-}$Hif1a$^{+/-}$Mb1-cre*, 4 *Vhl$^{-/-}$Hif1a$^{-/-}$Mb1-cre* and 7 *Vhl$^{+/-}$Hif1a$^{+/+}$Mb1-cre* biologically independent mice; data are pooled from two independent experiments. Symbols represent individual mice, bars means ± S.D.

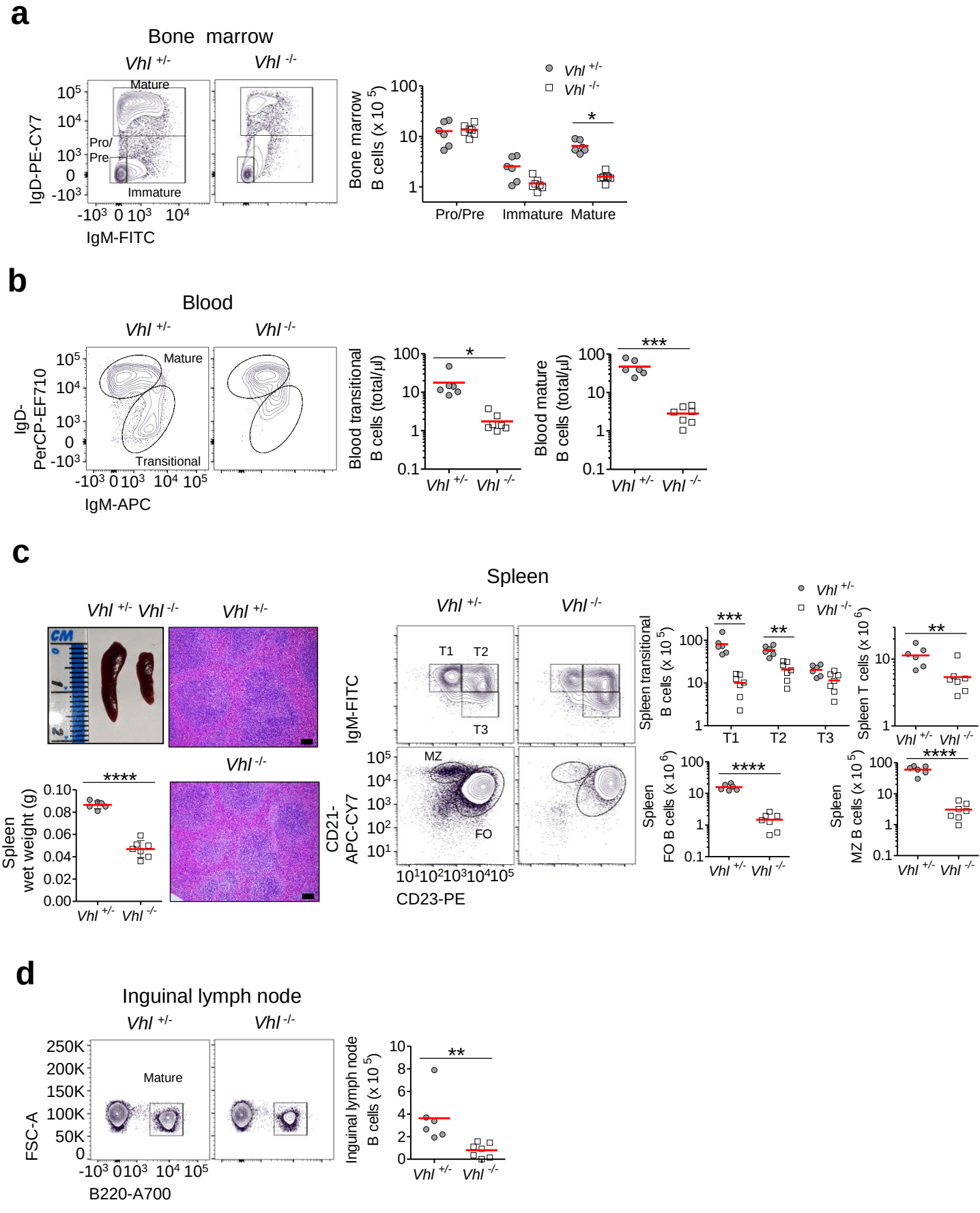

Supplementary Figure 4

B cell autonomous defects caused by loss of VHL lead to severe peripheral B cell lymphopenia

Flow cytometry showing the gating and absolute numbers of donor *Vhl*$^{+/-}$*Mb1-cre* and *Vhl*$^{-/-}$*Mb1-cre* B cells recovered from sub-lethally irradiated muMt^{-} recipient mice**,** 8 weeks after reconstitution from;
(a) BM
(b) Blood

Supplementary Figure 4

(c) Spleen, displayed; mean spleen wet weight and representative images of whole spleens and structure by hematoxylin and eosin staining (Scale-bar 100 μm) from muMt$^-$ recipient mice reconstituted with *Vhl*$^{+/-}$*Mb1-cre* or *Vhl*$^{-/-}$*Mb1-cre* BM. Note, muMt$^-$ spleens are typically half the weight of WT spleens owing to a lack of lymphoid cellularity. Here, wet weight is increased in muMt$^-$ spleens reconstituted with control BM due to increased B and T lymphocyte occupancy that is not seen in *Vhl*$^{-/-}$*Mb1-cre* reconstituted spleens. Total T cells gated as CD3$^+$.
(a-d) Gated as in Figure 1.
(a,c) **P*<0.05, ***P*<0.01, ****P*<0.001 two-way ANOVA Bonferroni post-test.
(b,c,d) **P*<0.05, ***P*<0.01, ****P*<0.001, *****P*<0.0001 unpaired two-sided *t* test.
(a-d) *n*=6 *Vhl*$^{+/-}$*Mb1-cre* and 7 *Vhl*$^{-/-}$*Mb1-cre* biologically independent mice from one experiment. Symbols represent individual mice, bars means ± S.D.

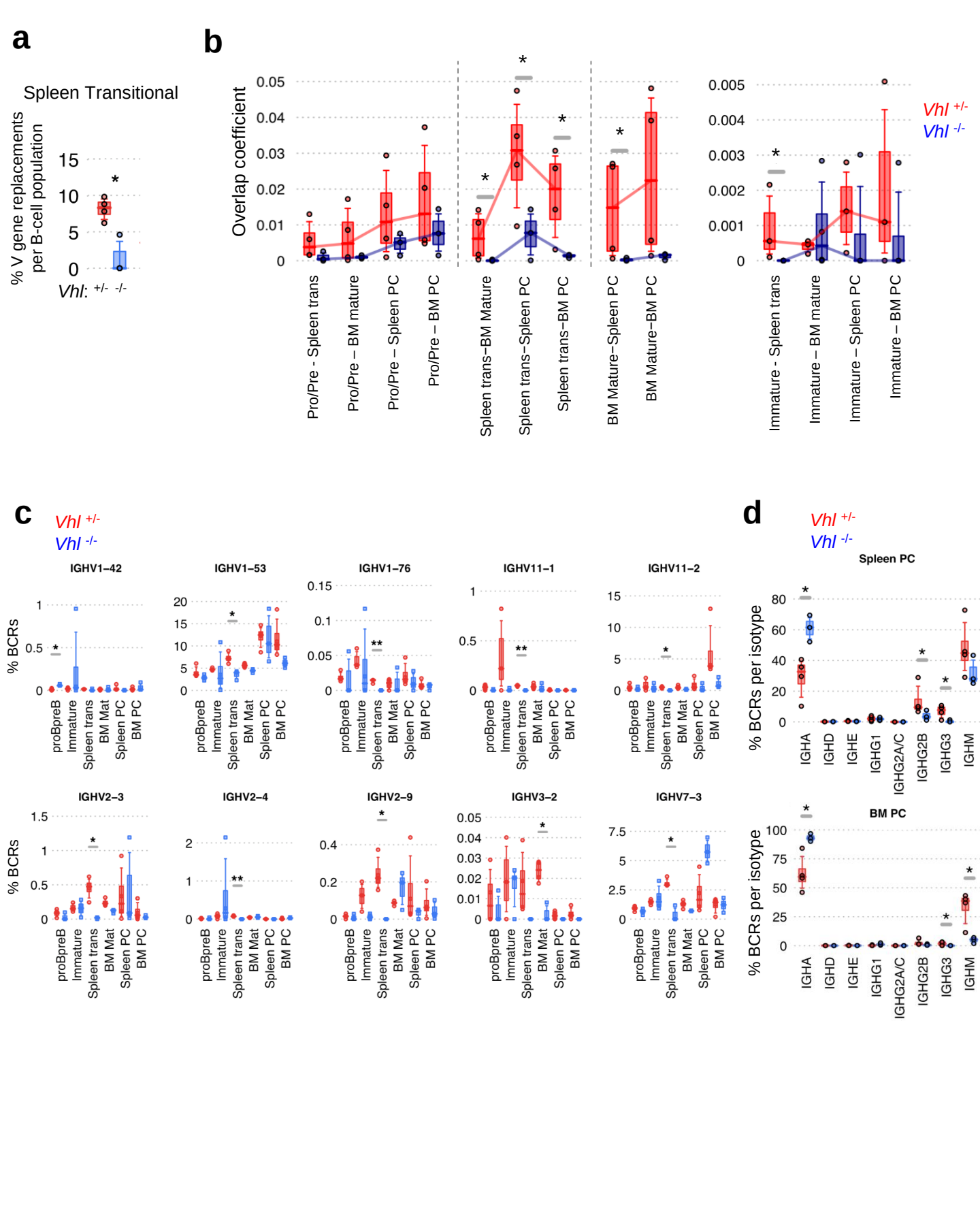

Supplementary Figure 5

HIF-1α activation leads to cell-intrinsic defects in the formation of the B cell repertoire

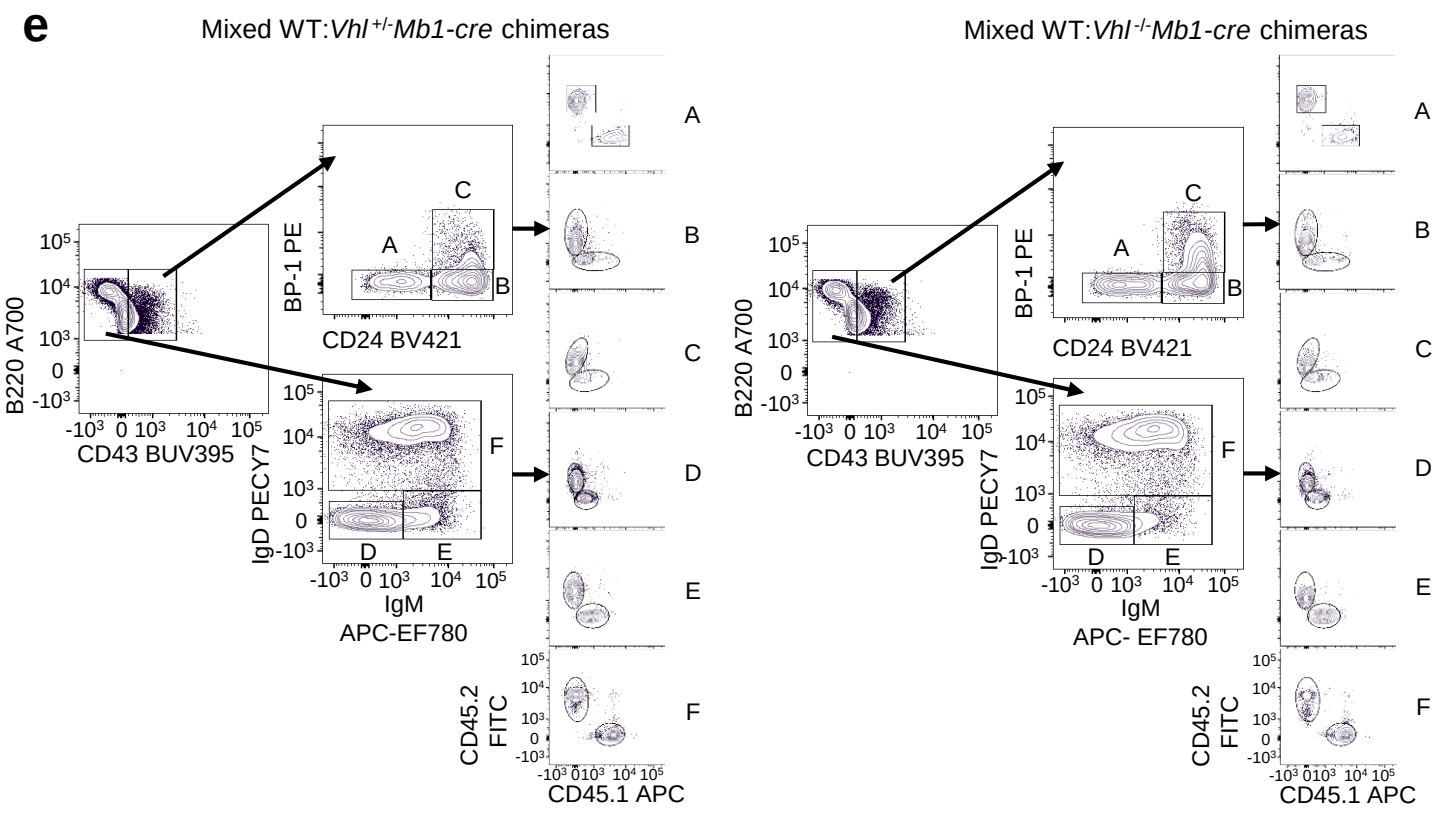

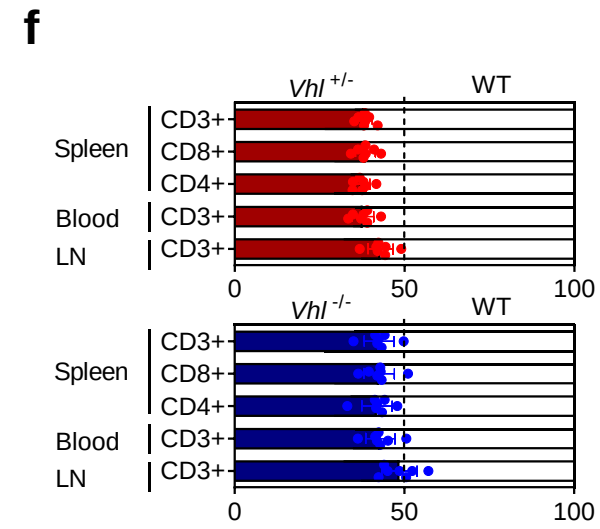

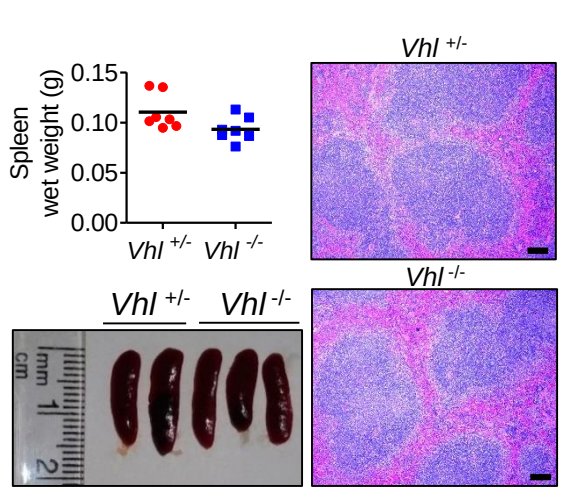

Supplementary Figure 5

(a) High-throughput detection of *IgHV* secondary rearrangements in *Vhl*$^{+/-}$*Mb1-cre* and *Vhl*$^{-/-}$*Mb1-cre* spleen transitional B cells (RNA), gated as in Figure 3a. **P*<0.05 one-sided Wilcoxon tests.
(b) Clonal overlap coefficients generated by calculating the probability that an overlap of BCR sequences between early (Pro-B/Pre-B, immature, transitional) and late (mature, plasma cells) developmental subsets can happen by chance. Left panel; RNA samples, trans= transitional, BM= bone marrow, PC = plasma cells (B220^{-}CD138^{+}). Right panel; DNA samples. Gated as in Figure 3a. **P*<0.05 one-sided Wilcoxon-tests.
(c) V gene usages that are differentially utilised between *Vhl*$^{+/-}$*Mb1-cre* (red) and *Vhl*$^{-/-}$*Mb1-cre* (blue) B cells. Plasma cells gated on B220^{-}CD138^{+}. **P*<0.05, ***P*<0.005 multivariate ANOVA.
(d) Percentage of BCRs per isotype between *Vhl*$^{+/-}$*Mb1-cre* (red) and *Vhl*$^{-/-}$*Mb1-cre* (blue) plasma cells (B220^{-}CD138^{+}). **P*<0.05 one-sided Wilcoxon-tests.
(a-d) Graphs; box lines show the 25th, 50th and 75th percentiles; whiskers show the 10th and 90th percentiles. Symbols represent individual mice. *n*=4 biologically independent mice per genotype, from one experiment.
(e) Gating strategy for the analysis of BM B cells from the mixed BM chimeras in Figure 3c.
(f) The relative proportion of CD3^{+}, CD4^{+} and CD8^{+} T cells in spleens and CD3^{+} T cells in blood and ILNs, from mixed BM chimeras. *n*=7 biologically independent mice per genotype, data are representative of two independent experiments. Filled columns; mean %CD45.2 *Vhl*$^{+/-}$*Mb1-cre* or *Vhl*$^{-/-}$*Mb1-cre* B cells, clear columns; mean %CD45.1 WT B cells, error bars S.D. Symbols represent individual mice.
(g) Mean spleen wet weight and representative images of whole spleens and structure by haematoxylin and eosin staining from mixed WT:*Vhl*$^{+/-}$*Mb1-cre* and mixed WT:*Vhl*$^{-/-}$*Mb1-cre* mice. Scale-bar 100 μm. *n*=7 biologically independent mice per genotype, data are representative of two independent experiments. Symbols represent individual mice, bars means ± S.D.

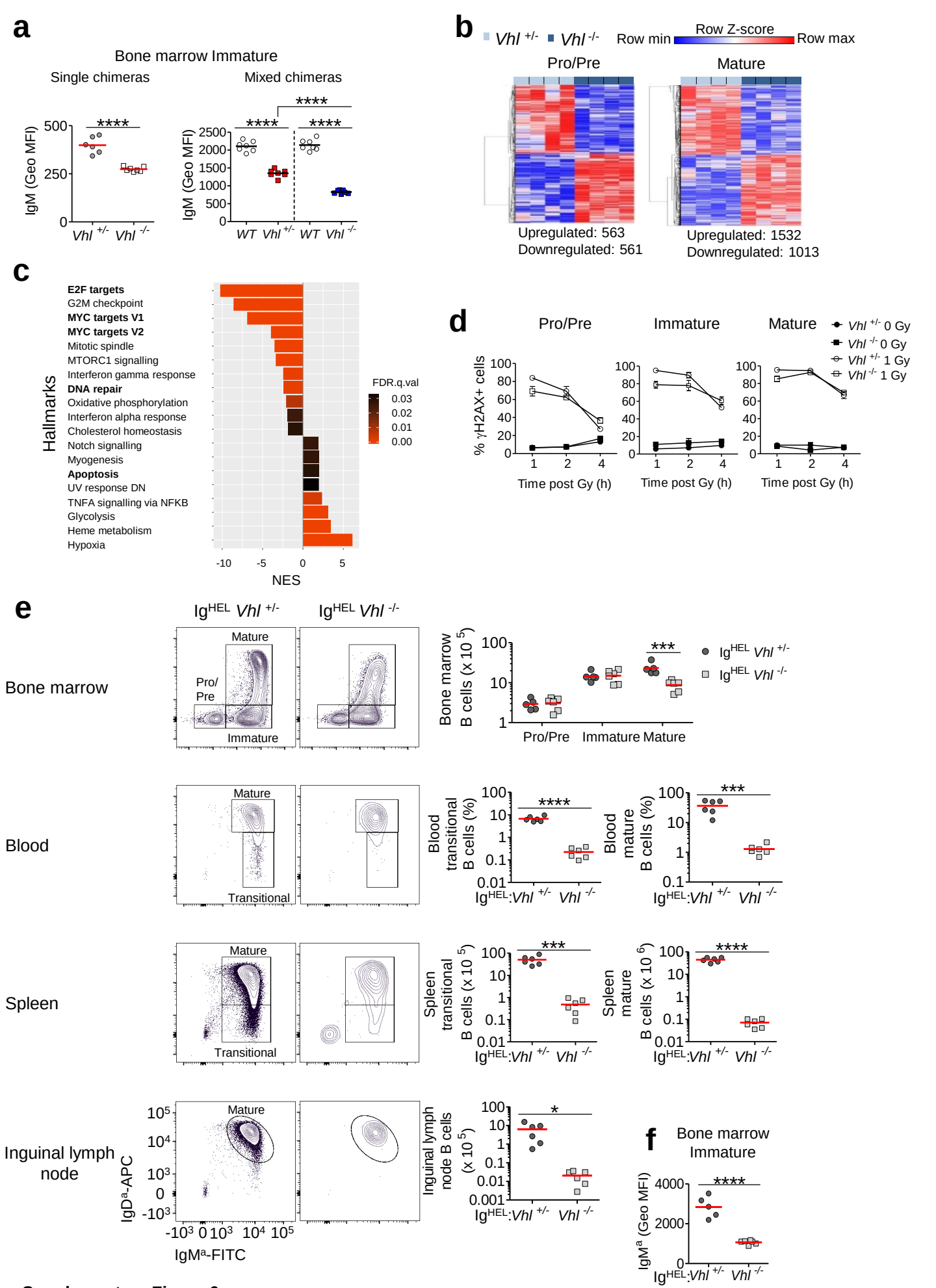

Supplementary Figure 6

***Vhl* loss leads to defects in B cell developmental processes**

Supplementary Figure 6

(a) Surface (s)IgM expression (Geo MFI), by flow cytometry, on donor *Vhl*$^{+/-}$*Mb1-cre* and *Vhl*$^{-/-}$*Mb1-cre* immature B cells recovered from **(left panel)** single chimeras described and gated as in Supplementary figure 4, and **(right panel)** mixed chimeras, described and gated as in Figure 3c. sIgM expression on immature B cells was not rescued in single or mixed *Vhl*$^{-/-}$*Mb1-cre* BM chimeras when compared to controls, indicating a cell-intrinsic effect. Note reduced IgM expression on *Vhl*$^{+/-}$*Mb1-cre* immature B cells compared to WT is due to the lack of one *mb-1* allele, replaced by *cre*. (left panel) ****P<0.0001 unpaired two-sided *t*-test, n=6 *Vhl*$^{+/-}$*Mb1-cre* and 7 *Vhl*$^{-/-}$*Mb1-cre* biologically independent mice from one experiment. (Right panel) ****P<0.0001 one-way ANOVA Tukey post-test, n=7 biologically independent mice per genotype, data are representative of two independent experiments. Symbols represent individual mice, bars means ± S.D.
(b) Heatmaps of differentially expressed genes (BH adjusted P value<0.05) in sorted Pro-B, Pre-B and mature B cells from *Vhl*$^{-/-}$*Mb1-cre* and *Vhl*$^{+/-}$*Mb1-cre* mice (described and gated as in Figures 4f-g). Columns represent individual mice.
(c) Gene set enrichment analysis (GSEA) of differentially expressed genes in *Vhl*$^{-/-}$*Mb1-cre* immature B cells when compared to *Vhl*$^{+/-}$*Mb1-cre* immature B cells (gated as in Figures 4e-g). A significant enrichment was defined as having a FDR $q \leq 0.05$.
(b-c) n=4 biologically independent mice per genotype, from one experiment.
(d) Percentage γH2AX+ *Vhl*$^{+/-}$*Mb1-cre* or *Vhl*$^{-/-}$*Mb1-cre* BM B cells, detected by flow cytometry, at 1, 2 and 4 h post 1 Gy radiation. 4x10^6 BM cells received 1 Gy X-ray radiation and were harvested at the respective time points. Gated as Pro-B, Pre-B B220$^+$IgM$^-$IgD$^-$, immature B220$^+$IgM$^+$IgD$^-$, mature B220$^+$IgM$^+$IgD$^+$. ns two-way ANOVA Bonferroni post-test. n=4 biologically independent mice per genotype, data are representative of two independent experiments. Error bars, S.E.M.
(e) Flow cytometry showing the gating and absolute numbers of B cells in BM, blood, spleens and ILNs of Ig^{HEL}*Vhl*$^{+/-}$*Mb1-cre* and Ig^{HEL}*Vhl*$^{-/-}$*Mb1-cre* mice. Gated on Pro-B, Pre-B B220$^+$IgM^{a-}IgD^{a-}, immature and transitional B220$^+$IgM^{a+}IgD^{a-} and mature B220$^+$IgM^{a+}IgD^{a+}. ***P<0.001 two-way ANOVA Bonferroni post-test, *P<0.05, ***P<0.001, ****P<0.0001 unpaired two-sided *t* test. n=5 Ig^{HEL}*Vhl*$^{+/-}$*Mb1-cre* (BM), 6 Ig^{HEL}*Vhl*$^{+/-}$*Mb1-cre* (blood, spleen, ILN) and 6 Ig^{HEL}*Vhl*$^{-/-}$*Mb1-cre* biologically independent mice, data are representative of two independent experiments. Symbols represent individual mice, bars means ± S.D.
(f) sIgM expression (Geo MFI), by flow cytometry, on Ig^{HEL}*Vhl*$^{+/-}$*Mb1-cre* and Ig^{HEL}*Vhl*$^{-/-}$*Mb1-cre* immature B cells, gated as in (e). ****P<0.0001 unpaired two-sided *t*-test. n=5 Ig^{HEL}*Vhl*$^{+/-}$*Mb1-cre and* 6 Ig^{HEL}*Vhl*$^{-/-}$*Mb1-cre* biologically independent mice, data are representative of two independent experiments. Symbols represent individual mice, bars means ± S.D.

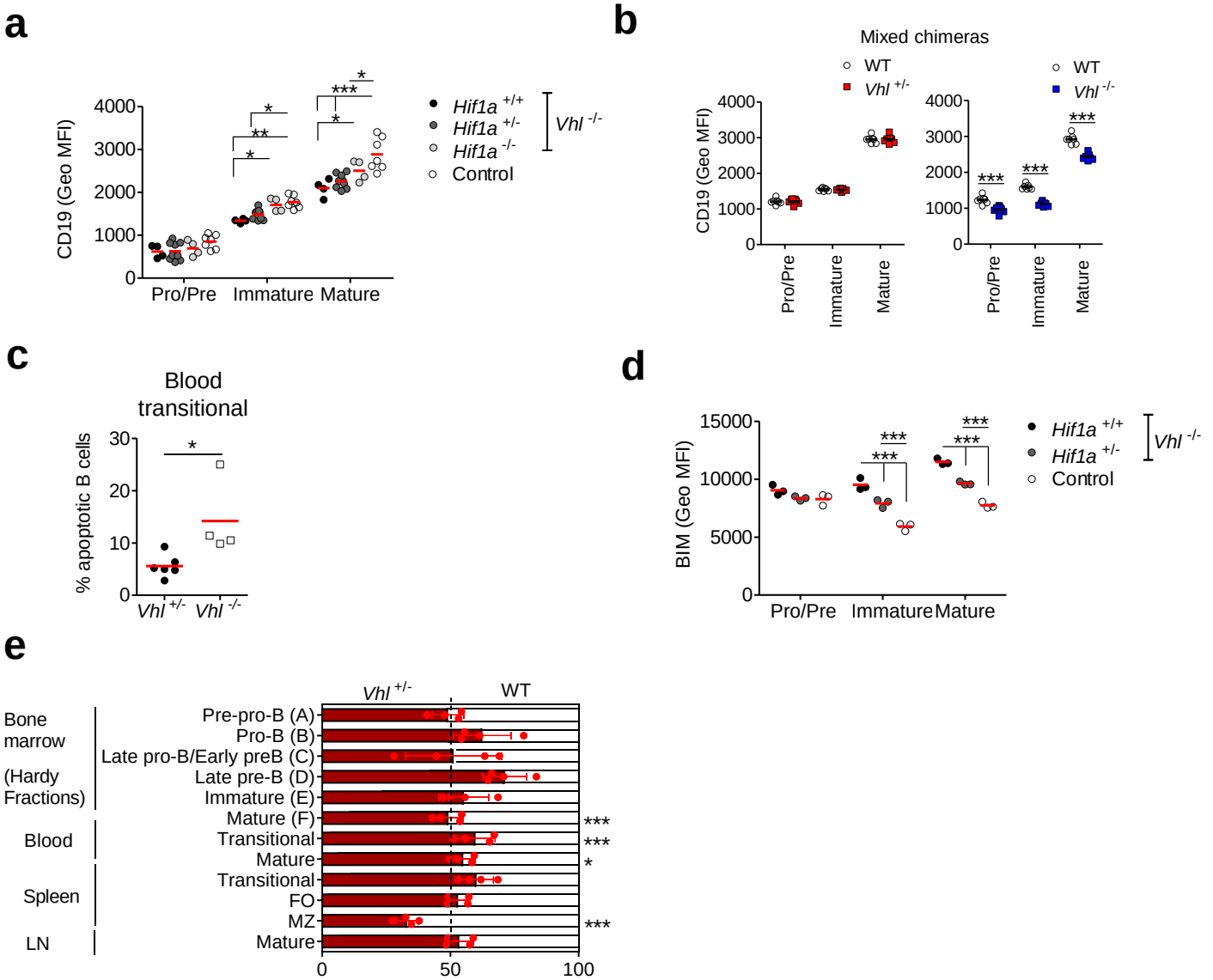

Supplementary Figure 7

HIF-1α activation leads to a cell-intrinsic reduction in CD19 expression and increased BIM expression and apoptosis in developing B cells

(a) CD19 expression (Geo MFI), by flow cytometry, on BM B cells from *Vhl*$^{-/-}$*Mb1-cre* mice carrying *Hif1a*$^{+/+}$, *Hif1a*$^{+/-}$ and *Hif1a*$^{-/-}$ alleles, and *Vhl*$^{+/-}$ *Hif1a*$^{+/+}$*Mb1-cre* control mice, gated as in Figure 2. **P*<0.05, ***P*<0.01, ****P*<0.001 two-way ANOVA Bonferroni post-test. *n*=4 *Vhl*$^{-/-}$*Hif1a*$^{+/+}$*Mb1-cre*, 9 *Vhl*$^{-/-}$*Hif1a*$^{+/-}$*Mb1-cre*, 4 *Vhl*$^{-/-}$*Hif1a*$^{-/-}$*Mb1-cre* and 7 *Vhl*$^{+/-}$*Hif1a*$^{+/+}$*Mb1-cre* biologically independent mice, data are pooled from two independent experiments.
(b) CD19 expression (Geo MFI), by flow cytometry, on donor BM B cells recovered from mixed chimeras described and gated as in Figure 3c. CD19 expression was low on *Vhl*$^{-/-}$*Mb1-cre* BM B cells from mixed WT:*Vhl*$^{-/-}$*Mb1-cre* BM chimeras compared to mixed WT:*Vhl*$^{+/-}$*Mb1-cre* BM B cells indicating a cell-intrinsic defect. ****P*<0.001 two-way ANOVA Bonferroni post-test. *n*=7 biologically independent mice per genotype, data are representative of two independent experiments.
(c) Percentage apoptotic blood transitional B cells from *Vhl*$^{+/-}$*Mb1-cre* and *Vhl*$^{-/-}$*Mb1-cre* mice, measured by PO-PRO-1 and 7-AAD staining, by flow cytometry. **P*<0.05 unpaired two-sided *t* test. *n*=6 *Vhl*$^{+/-}$*Mb1-cre* and 4 *Vhl*$^{-/-}$*Mb1-cre* biologically independent mice from one experiment.
(d) BIM expression (Geo MFI), by flow cytometry, on BM B cells from *Vhl*$^{-/-}$*Mb1-cre* mice carrying *Hif1a*$^{+/+}$ and *Hif1a*$^{+/-}$ alleles, and *Vhl*$^{+/-}$ *Hif1a*$^{+/+}$*Mb1-cre* control mice, gated as in Figure 1c. ****P*<0.001 two-way ANOVA Bonferroni post-test. *n*=3 biologically independent mice per genotype from a single experiment.
(e) The relative proportion of B cell subsets in lethally irradiated CD45.1 mice reconstituted for 8 weeks with 1:1 mixtures of CD45.1 WT and CD45.2 control *Vhl*$^{+/-}$*Mb1-cre* BM, ancillary to the experiment depicted in Figure 5d. Filled columns; mean %CD45.2, clear columns; mean %CD45.1. Error bars S.D.; reconstitution was rescued in *Vhl*$^{-/-}$*Mb1-cre* B cells with deleted BIM (Figure 5d;*Vhl*$^{-/-}$*Mb1-cre+Bcl2l11*$^{-/-}$) to a similar level to that seen here in control BM; comparison between *Vhl*$^{-/-}$*Mb1-cre+Bcl2l11*$^{-/-}$ and *Vhl*$^{+/-}$*Mb1-cre* BM by two-way ANOVA Bonferroni post-test, **P*<0.05,****P*<0.001, *n*=4 WT:*Vhl*$^{+/-}$*Mb1-cre* biologically independent mice. Data, representative of two independent experiments.
(a-e) Symbols represent individual mice, bars means ± S.D.

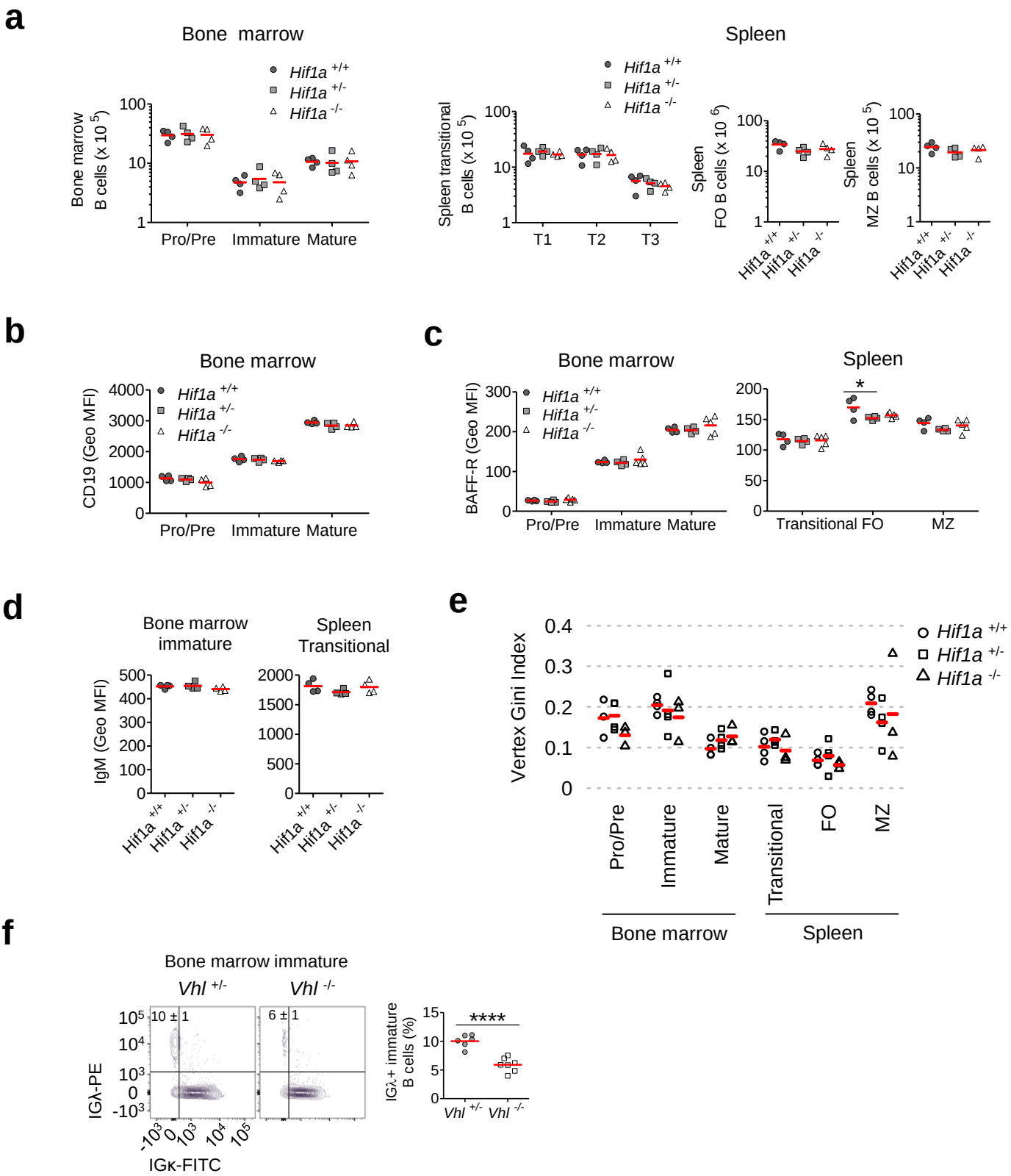

Supplementary Figure 8

Hif1a*$^{-/-}$*Mb1-cre **mice have a normal complement of B cells and** ***Vhl*$^{-/-}$*Mb1-cre*** **have cell-intrinsic alterations in IGλ+ usage**

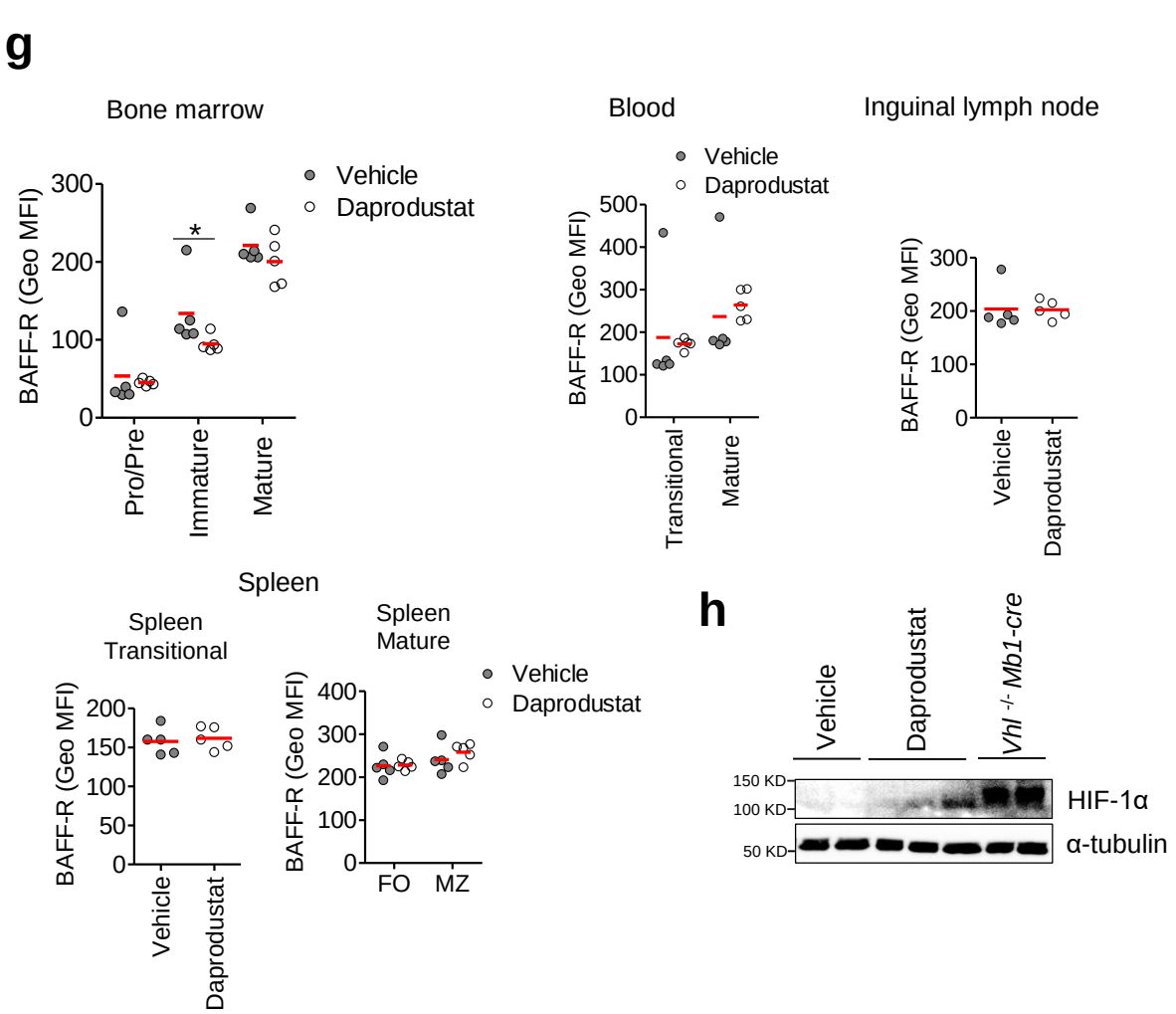

Supplementary Figure 8

(a) Enumeration of B cell subsets, by flow cytometry, from *Hif1a*$^{+/+}$*Mb1-cre*, *Hif1a*$^{+/-}$*Mb1-cre* and *Hif1a*$^{-/-}$*Mb1-cre* mice in BM and spleen. Two-way ANOVA Bonferroni post-test, one-way ANOVA Tukey post-test. *n*=4 biologically independent mice per genotype, data are representative of three independent experiments.
(b) Mean expression (Geo MFI) by flow cytometry of CD19 on *Hif1a*$^{+/+}$*Mb1-cre*, *Hif1a*$^{+/-}$*Mb1-cre* and *Hif1a*$^{-/-}$*Mb1-cre* BM B cells. Two-way ANOVA Bonferroni post-test. *n*=4 biologically independent mice per genotype, data are representative of two independent experiments.
(c) Mean BAFF-R expression (Geo MFI), by flow cytometry, on *Hif1a*$^{+/+}$*Mb1-cre*, *Hif1a*$^{+/-}$*Mb1-cre* and *Hif1a*$^{-/-}$*Mb1-cre* BM and spleen B cells. **P*<0.05 two-way ANOVA Bonferroni post-test. *n*=4 *Hif1a*$^{+/+}$*Mb1-cre*, 4 *Hif1a*$^{+/-}$*Mb1-cre*, 5 *Hif1a*$^{-/-}$*Mb1-cre* biologically independent mice from one experiment.
(d) sIgM expression (Geo MFI) on *Hif1a*$^{+/+}$*Mb1-cre*, *Hif1a*$^{+/-}$*Mb1-cre* and *Hif1a*$^{-/-}$*Mb1-cre* BM immature and spleen transitional B cells. One-way ANOVA Tukey post-test. *n*=4 biologically independent mice per genotype, data are representative of two independent experiments.
(e) Clonal analysis of *IgHV-D-J* RNA rearrangements from BM and spleen *Hif1a*$^{+/+}$*Mb1-cre*, *Hif1a*$^{+/-}$*Mb1-cre* and *Hif1a*$^{-/-}$*Mb1-cre* B cells, quantified using the Vertex Gini Index (See methods). B cells gated as in Figure 3a. MZ gated as B220^{+}IgM^{+}IgD^{+}CD23^{-}CD21^{+}. Bars medians, one-sided Wilcoxon-tests, *n*=4 *Hif1a*$^{+/+}$*Mb1-cre, 4 Hif1a*$^{+/-}$*Mb1-cre*, 3 *Hif1a*$^{-/-}$*Mb1-cre* biologically independent mice from one experiment.
(f) Flow cytometry illustrating the frequency of donor IGλ+ and IGκ+ *Vhl*$^{+/-}$*Mb1-cre* and *Vhl*$^{-/-}$*Mb1-cre* immature B cells (± S.D.) recovered from single chimeras described and gated as in Supplementary figure 4. *****P*<0.0001 unpaired two-sided *t*-test. *n*=6 *Vhl*$^{+/-}$*Mb1-cre* and 7 *Vhl*$^{-/-}$*Mb1-cre* biologically independent mice from one experiment.
(g) Mean BAFF-R expression (Geo MFI), by flow cytometry, in B cells from C57BL/6J mice treated for 8 days with vehicle (2% DMSO, PBS) or 30 mg/kg daprodustat every 12 h. **P*<0.05 two-sided Mann-Whitney U test. *n*=5 biologically independent mice per group from one experiment.
(h) Immunoblot of HIF-1α protein in homogenized ILNs from C57BL/6J mice treated with vehicle (*n*=2) and daprodustat (*n*=3) as in (g) and *Vhl*$^{-/-}$*Mb1-cre* (*n*=2) biologically independent mice from one experiment. Lower levels of HIF-1α are observed in ILNs of daprodustat-treated mice compared to *Vhl*$^{-/-}$*Mb1-cre* mice. α-tubulin was used as the loading control. In interpreting this result, it is important to note that in ILNs from daprodustat-treated mice HIF-1α will be activated in other cell types besides B cells, and that this represents evaluation at a single time point, in a single experiment and in a single tissue.
(a-d,f,g) Gated as in Figure 1, **(a-g)** Symbols represent individual mice, bars means ± S.D.

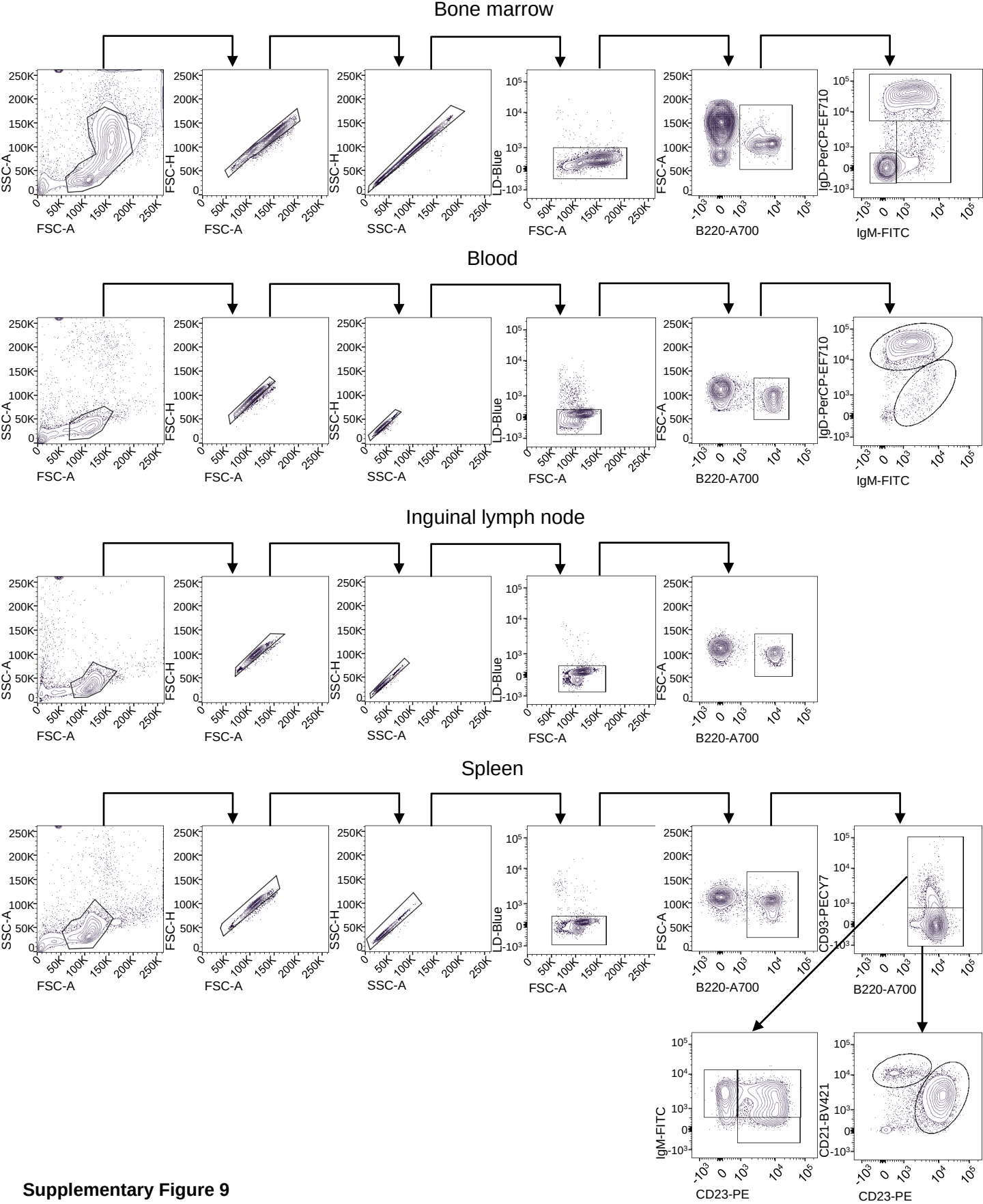

Supplementary Figure 9

Gating strategies for flow cytometry and cell sorting experiments

Cells were first selected based on FSC-A x SSC-A, then singlets were gated on as FSC-A x FSC-H, SSC-A x SSC-H, then FSC-A x LIVE/DEAD (LD) stain was used to exclude dead cells, then FSC-A x B220+ were gated on to identify B cells. Further gates were then applied to identify sub-populations of B cells in different lymphoid tissues, as described and shown in the main figures. Displayed are general gating strategies used for all figures generated from flow cytometry data collection using control mice from Figures 1c-f as an example in; bone marrow, blood, ILNs and spleens. Gates used to identify sub-populations of B cells that differed from those shown here are provided in the relevant figures.

Supplementary table 1: List of flow cytometry antibodies

Antibody	Reactivity	Clone	Dilution	Company	Catalogue Number
Mouse anti-AKT (pS473) Alexa Fluor 488	Mouse/human	M89-61	1:10	BD Biosciences	560404
Bim (C34C5) Alexa (R) 647	mouse/human/rat	C34C5	1:25	Cell Signaling	10408
CD11b PE-Cyanine7	mouse	M1/70	1:600	Thermo Fisher Scientific (eBioscience)	25-0112-82
CD138 Brilliant Violet 421	mouse	281-2	1:400	BD Biosciences	562610
CD19 APC	mouse	6D5	1:400	Biolegend	115512
CD19 PerCP-Cyanine5.5	mouse	1D3	1:100	Thermo Fisher Scientific (eBioscience)	45-0193-82
CD21/CD35 APC/CY7	mouse	7E9	1:200	Biolegend	123417
CD21/CD35 Brilliant Violet 421	mouse	7E9	1:400	Biolegend	123421
CD21/CD35 Brilliant Violet 605	mouse	7G6	1:400	BD Biosciences	563176
CD23 APC/CY7	mouse	B3B4	1:400	Biolegend	101630
CD23 PE	mouse	B3B4	1:400	Thermo Fisher Scientific (eBioscience)	12-0232-82
CD23 PerCP-eFluor 710	mouse	B3B4	1:400	Thermo Fisher Scientific (eBioscience)	46-0232-80
CD24 Brilliant Violet 421	mouse	M1/69	1:400	Biolegend	101826
CD24 PerCP-Cyanine5.5	mouse	M1/69	1:200	Biolegend	101823
CD249 (BP-1) PE	mouse	6C3	1:400	Thermo Fisher Scientific (eBioscience)	12-5891-82
CD268 (BAFF-R) APC	mouse	7H22-E16	1:200	Thermo Fisher Scientific (eBioscience)	17-5943-80
CD3 Alexa Fluor 700	mouse	17A2	1:200	Thermo Fisher Scientific (eBioscience)	56-0032-80
CD3 PerCP-eFluor 710	mouse	Ebio500a2	1:400	Thermo Fisher Scientific (eBioscience)	46-0033-82
CD4 Alexa Fluor 700	mouse	GK1.5	1:200	Thermo Fisher Scientific (eBioscience)	56-0041-80
CD4 Brilliant Violet 421	mouse	GK1.5	1:400	Biolegend	100437
CD4 PerCP-Cyanine5.5	mouse	RM4-5	1:100	Thermo Fisher Scientific (eBioscience)	45-0042-80
CD43 BUV395	mouse	S7	1:200	BD Biosciences	740224
CD45.1 APC	mouse	A20	1:400	Thermo Fisher Scientific (eBioscience)	17-0453-81
CD45.1 FITC	mouse	A20	1:400	Thermo Fisher Scientific (eBioscience)	11-0453-82
CD45.2 FITC	mouse	104	1:400	Biolegend	109806
CD45R (B220) Alexa Fluor 700	mouse/human	RA3-6B2	1:200	Thermo Fisher Scientific (eBioscience)	56-0452-82
CD45R (B220) APC	mouse/human	RA3-6B2	1:400	Thermo Fisher Scientific (eBioscience)	17-0452-82
CD45R (B220) Brilliant Violet 421	mouse/human	RA3-6B2	1:200	Biolegend	103240
CD45R (B220) Brilliant Violet 605	mouse/human	RA3-6B2	1:100	BD Biosciences	563708
CD45R (B220) PE	Mouse/human	RA3-6B2	1:800	Thermo Fisher Scientific (eBioscience)	12-0452-82
CD5 Brilliant Violet 421	mouse	53-7.3	1:50	Biolegend	100617
CD8a FITC	mouse	53-6.7	1:400	Thermo Fisher Scientific (eBioscience)	11-0081-82
CD93 PE-Cyanine7	mouse	AA4.1	1:400	Thermo Fisher Scientific (eBioscience)	25-5892-82
EF5 Alexa Fluor 488	-	ELK3-51	1:27	Merck (Millipore)	EF5-30A4
EF5 Cy5	-	ELK3-51	1:50	Merck (Millipore)	EF5012
Histone H2A.X PE	mouse/human/rat/monkey	D17A3	1:50	Cell Signaling	53604S
IgD APC	mouse	11-26c	1:400	Thermo Fisher Scientific (eBioscience)	17-5993-82
IgD APC-eFluor 780	mouse	11-26c	1:400	Thermo Fisher Scientific (eBioscience)	47-5993-82
IgD PE-Cyanine7	mouse	11-26c	1:400	Thermo Fisher Scientific (eBioscience)	25-5993-82
IgD PerCP-eFluor 710	mouse	11-26c	1:400	Thermo Fisher Scientific (eBioscience)	46-5993-80
IgD^{a} APC	mouse	REA484	1:20	Miltenyi Biotec	130-107-134
IgM APC	mouse	II/41	1:400	Thermo Fisher Scientific (eBioscience)	17-5790-82
IgM APC-eFluor 780	mouse	II/41	1:400	Invitrogen Thermo Fisher Scientific	47-5790-82
IgM Brilliant Violet 421	mouse	R6-60.2	1:200	BD Horizon	562595
IgM FITC	mouse	eB121-15F9	1:400	Thermo Fisher Scientific (eBioscience)	11-5890-85
IgM PE	mouse	eB121-15F9	1:400	Thermo Fisher Scientific (eBioscience)	12-5890-82
IgM^{a} FITC	mouse	MA-69	1:400	Biolegend	408606
Kappa FITC	mouse	187.1	1:600	SouthernBiotech	1170-2S
Lambda PE	mouse	JC5-1	1:400	SouthernBiotech	1175-09

Supplementary table 2: RNA BCR amplification primer sequences

Barcoded RT-PCR B-cell receptor IsoTyper amplification from RNA from mice

Reverse RT primer mix (10uM per primer): Mixed in equimolar amounts to a final concentration of 10uM per primer for the PCR reaction.

Primer ID	Primer
MusM_IGHGA_BC	GATACGGCGACCAATGTNNNNTNNNNTNNNNCAGGGACCAAGGGATAGAC
MusM_IGHGB_BC	GATACGGCGACCAATGTNNNNTNNNNTNNNNCAGGGGCCAGTGGATAG
MusM_IGHA_BC	GATACGGCGACCAATGTNNNNTNNNNTNNNNTGTCAGTGGGTAGATGGTG
MusM_IGHM_BC	GATACGGCGACCAATGTNNNNTNNNNTNNNNCATGGCCACCAGATTCT
MusM_IGHE_BC	GATACGGCGACCAATGTNNNNTNNNNTNNNNAAGGGGTAGAGCTGAGGG
MusM_IGHD_BC	GATACGGCGACCAATGTNNNNTNNNNTNNNNGGCTTTGCACTCTGAGAG

PCR reverse primer:

Primer ID	Primer
UNIB	GATACGGCGACCAATGT

Forward primer mix (10uM per primer): this refers to the current forward primers used in the PCR reaction that bind to FR1 region of mouse *IgH* sequences: Mixed in equimolar amounts to a final concentration of 10uM per primer for the PCR reaction:

Primer ID	Primer sequence*	
VH-for11	CAGATKCAGCTTMAGGAGTC	
VH-for13	CAGGTTCACCTACAACAGTC	
VH-for15	GARGTGMAGCTGKTGGAGAC	
VH-for2	CAGGTGCAAMTGMAGSAGTC	Group 1 forward primers
VH-for5	GAKGTGCAGCTTCAGSAGTC	
VH-for8	GAGGTGMAGCTASTTGAGWC	
VH-for1	GAGGTTCDSCTGCAACAGTY	
VH-for12	CAGGCTTATCTGCAGCAGTC	
VH-for14	CAGGTGCAGCTTGTAGAGAC	Group 2 forward primers
VH-for3	GAVGTGMWGCTGGTGGAGTC	
VH-for7	CAGRTCCAACTGCAGCAGYC	

* Using standard ambiguity codes

Supplementary table 3: DNA BCR amplification primer sequences

Primer ID	Primer sequence*	
VH-for11	CAGATKCAGCTTMAGGAGTC	
VH-for13	CAGGTTCACCTACAACAGTC	
VH-for15	GARGTGMAGCTGKTGGAGAC	
VH-for2	CAGGTGCAAMTGMAGSAGTC	Group 1 forward primers
VH-for5	GAKGTGCAGCTTCAGSAGTC	
VH-for8	GAGGTGMAGCTASTTGAGWC	
VH-for1	GAGGTTCDSCTGCAACAGTY	
VH-for12	CAGGCTTATCTGCAGCAGTC	
VH-for14	CAGGTGCAGCTTGTAGAGAC	Group 2 forward primers
VH-for3	GAVGTGMWGCTGGTGGAGTC	
VH-for7	CAGRTCCAACTGCAGCAGYC	
JH-1_reverse	CTTACCTGAGGAGACGGTGA	J reverse primers
JH-2_reverse	CTTACCTGCAGAGACAGTGA	

* Using standard ambiguity codes

Burrows et al: Uncropped blots for Supplementary Figure 8h;

Displayed are uncropped blots without and with PVDF membrane containing the protein ladder (Precision Plus, Biorad), overlaid for molecular weight identification.

Please note that the PVDF membranes were cut in half so that HIF-α proteins and loading control proteins (α-tubulin) could be identified simultaneously.

Supplementary figure 8h

Uncropped blots

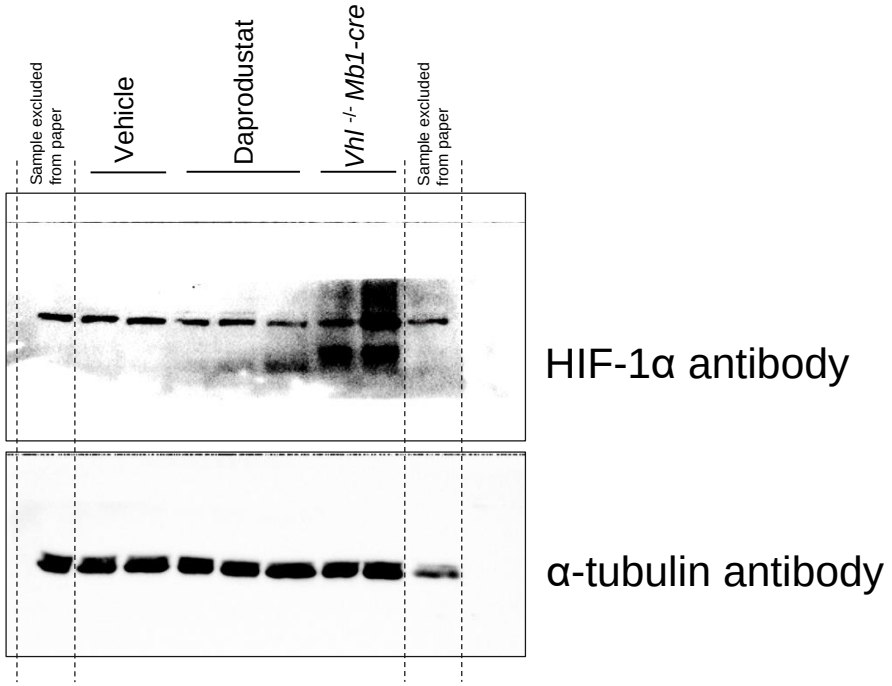

Uncropped blots with PVDF membrane containing the protein ladder (Precision Plus, Biorad), overlaid

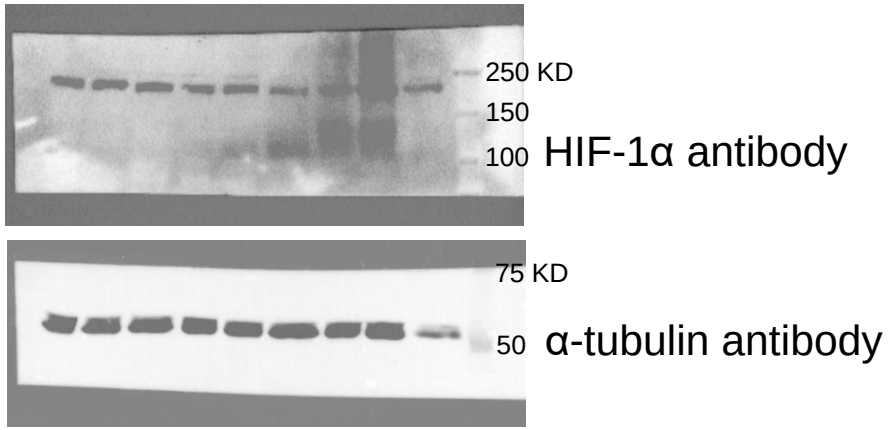

Burrows et al: Uncropped blots for Supplementary Figures 3a-c;

Displayed are uncropped blots without and with PVDF membrane containing the protein ladder (Precision Plus, Biorad), overlaid for molecular weight identification.

Please note that the PVDF membranes were cut in half so that HIF-α proteins and loading control proteins (β-actin) could be identified simultaneously.

Supplementary figure 3a (Bone marrow)

Uncropped blots

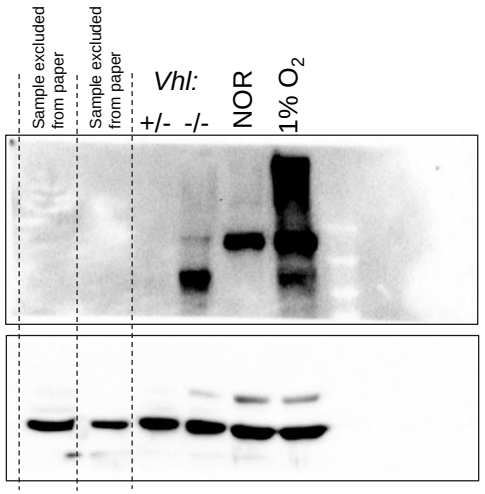

HIF-1α antibody

β-actin antibody

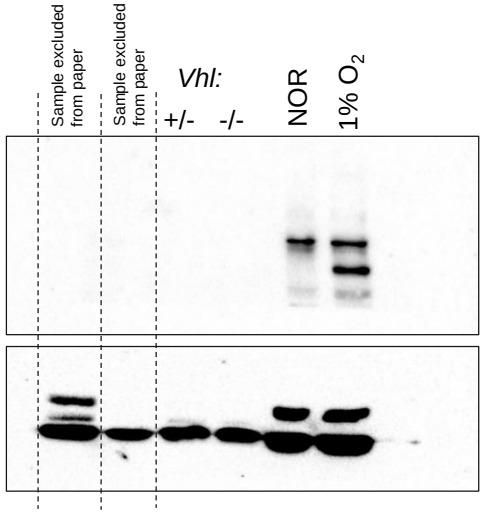

HIF-2α antibody

β-actin antibody

Uncropped blots with PVDF membrane containing the protein ladder (Precision Plus, Biorad), overlaid

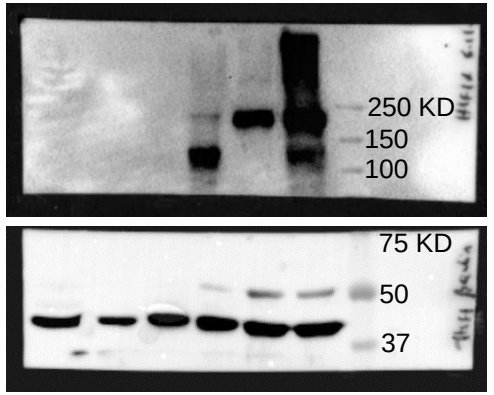

HIF-1α antibody

β-actin antibody

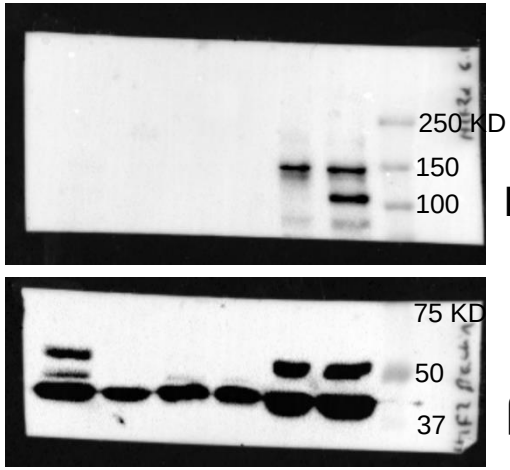

HIF-2α antibody

β-actin antibody

Supplementary figure 3a (Inguinal lymph node)

Uncropped blots

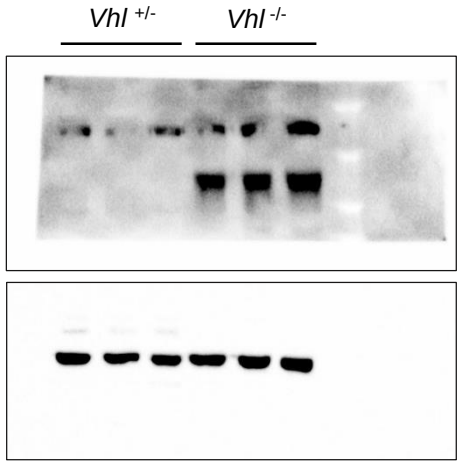

HIF-1α antibody

β-actin antibody

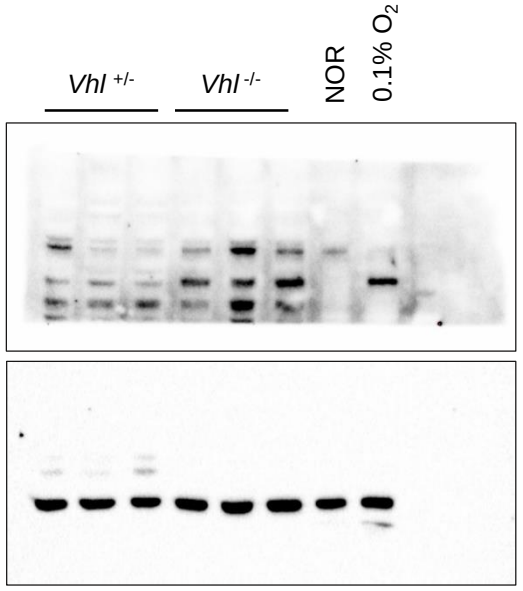

HIF-2α antibody

β-actin antibody

Uncropped blots with PVDF membrane containing the protein ladder (Precision Plus, Biorad), overlaid

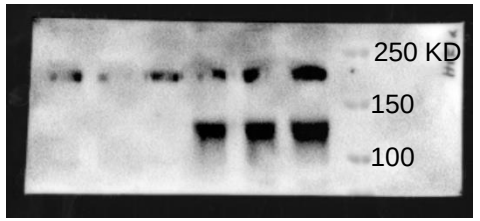

HIF-1α antibody

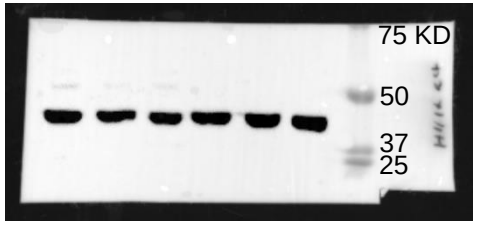

β-actin antibody

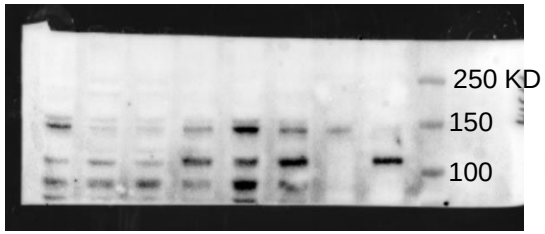

HIF-2α antibody

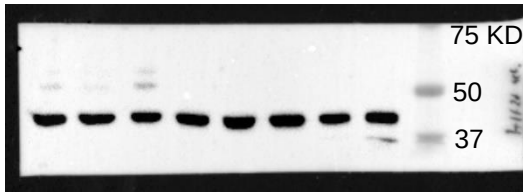

β-actin antibody

Uncropped blots

Uncropped blots with PVDF membrane containing the protein ladder (Precision Plus, Biorad), overlaid

Supplementary figure 3b

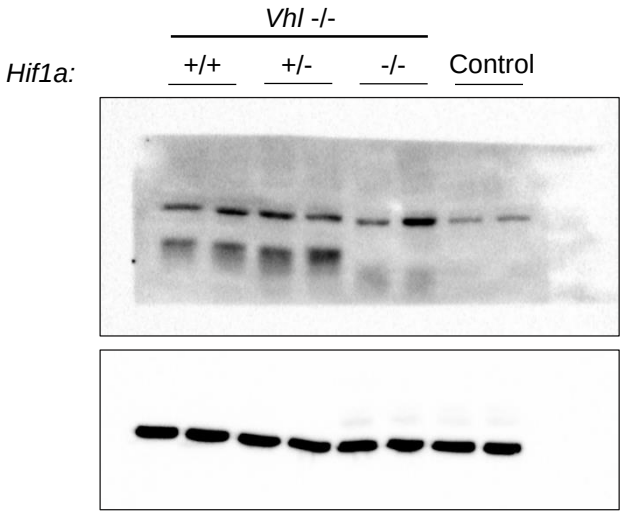

HIF-1α antibody

β-actin antibody

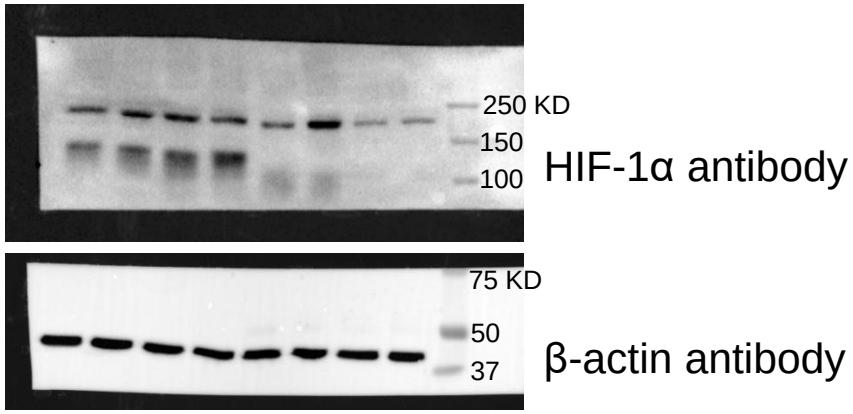

HIF-1α antibody

β-actin antibody

Supplementary figure 3c

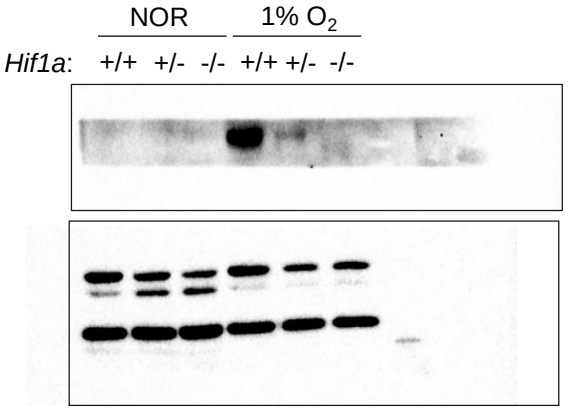

HIF-1α antibody

β-actin antibody

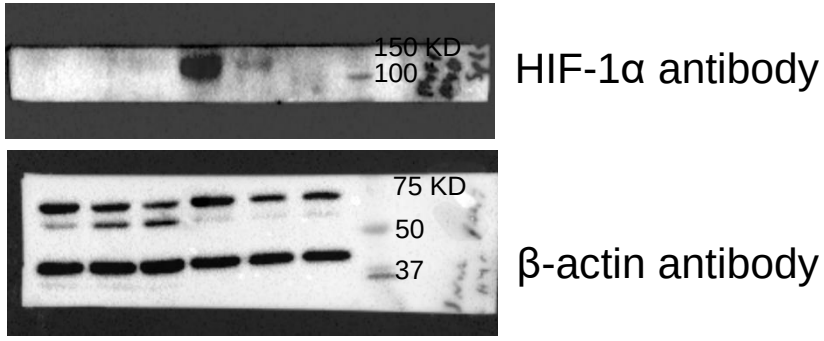

HIF-1α antibody

β-actin antibody

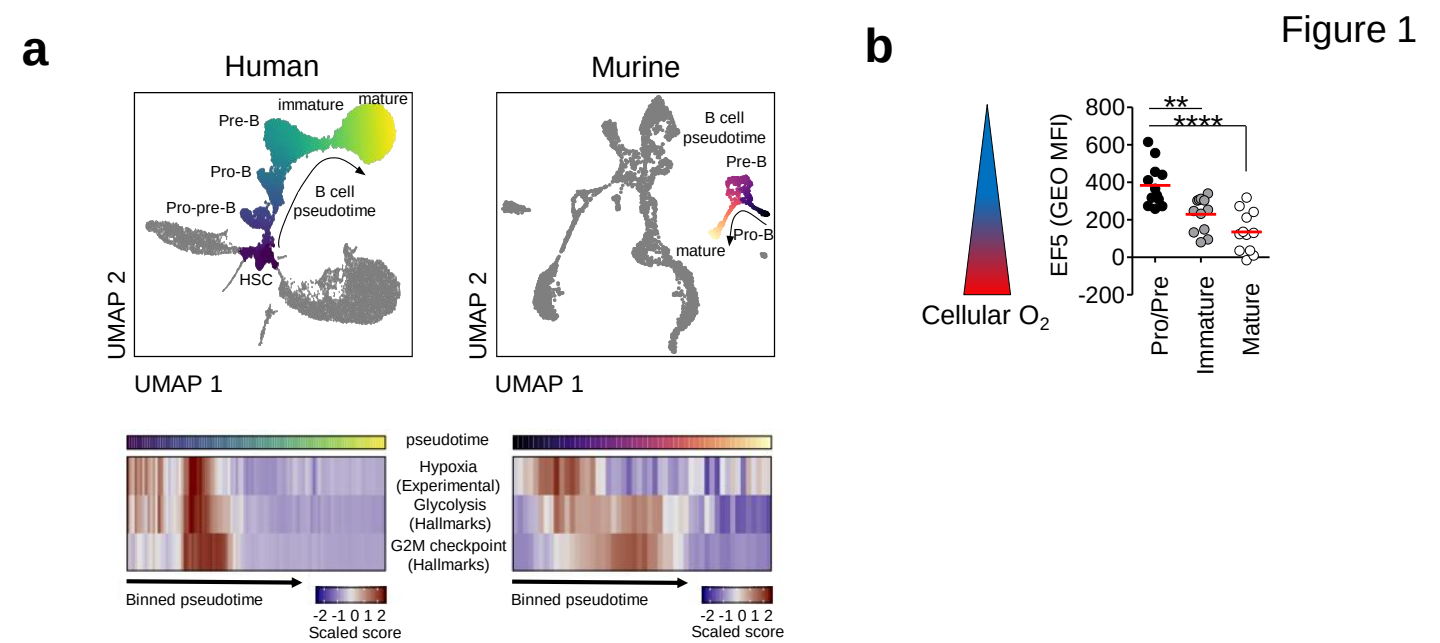
a
Human
Murine
immature
mature
Pre-B
Pro-B
Pro-pre-B
HSC
B cell pseudotime
UMAP 2
UMAP 1
pseudotime
Hypoxia (Experimental)
Glycolysis (Hallmarks)
G2M checkpoint (Hallmarks)
Binned pseudotime
Scaled score
b
Cellular O2
EF5 (GEO MFI)
Pro/Pre
Immature
Mature

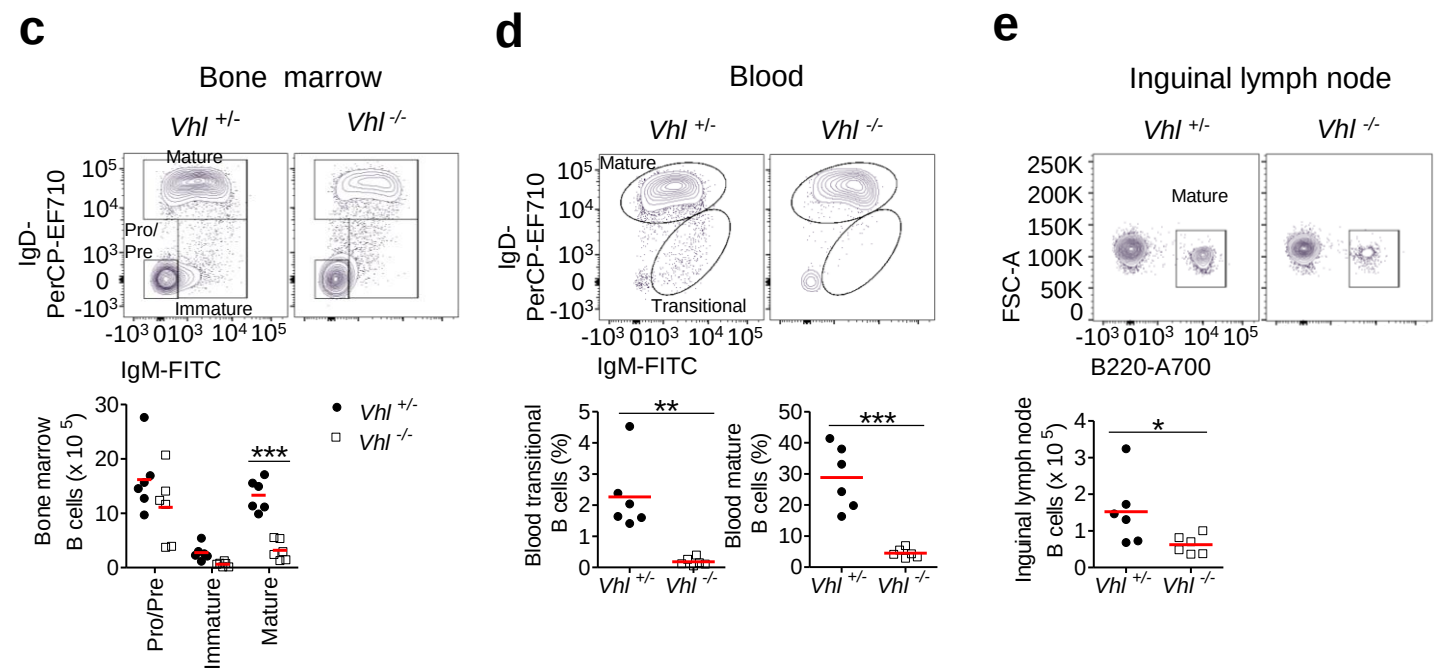
c
Bone marrow
Vhl +/-
Vhl -/-
IgD-PerCP-EF710
IgM-FITC
Mature
Pro/Pre
Immature
Bone marrow B cells (x 10 5)
d
Blood
Transitional
Blood transitional B cells (%)
Blood mature B cells (%)
e
Inguinal lymph node
FSC-A
B220-A700
Inguinal lymph node B cells (x 10 5)

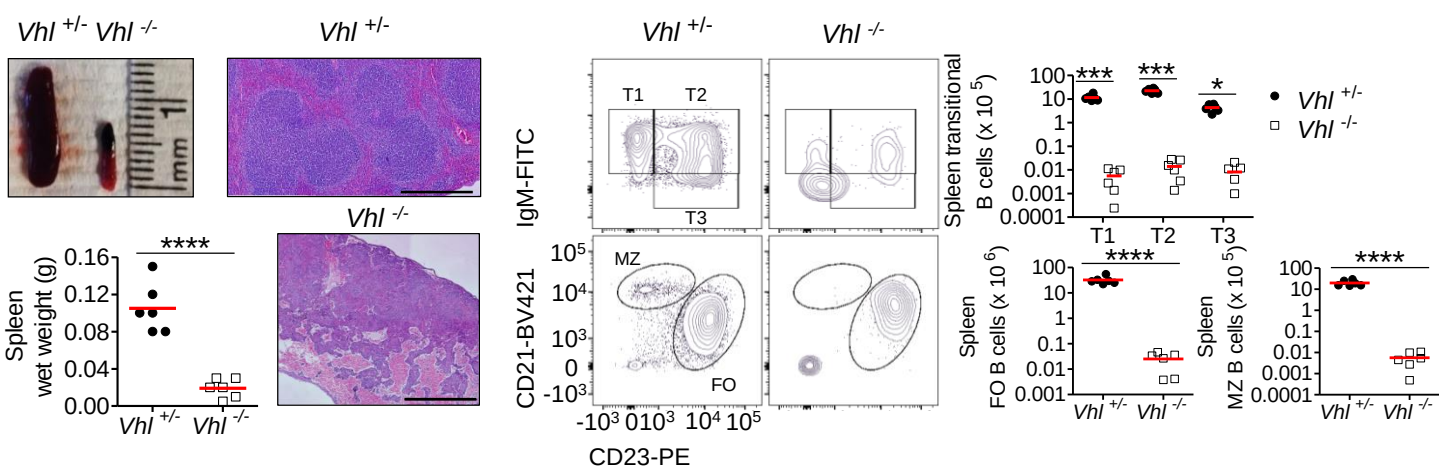
f
Spleen
Spleen wet weight (g)
IgM-FITC
CD23-PE
CD21-BV421
T1
T2
T3
MZ
FO
Spleen transitional B cells (x 10 5)
Spleen FO B cells (x 10 6)
Spleen MZ B cells (x 10 5)

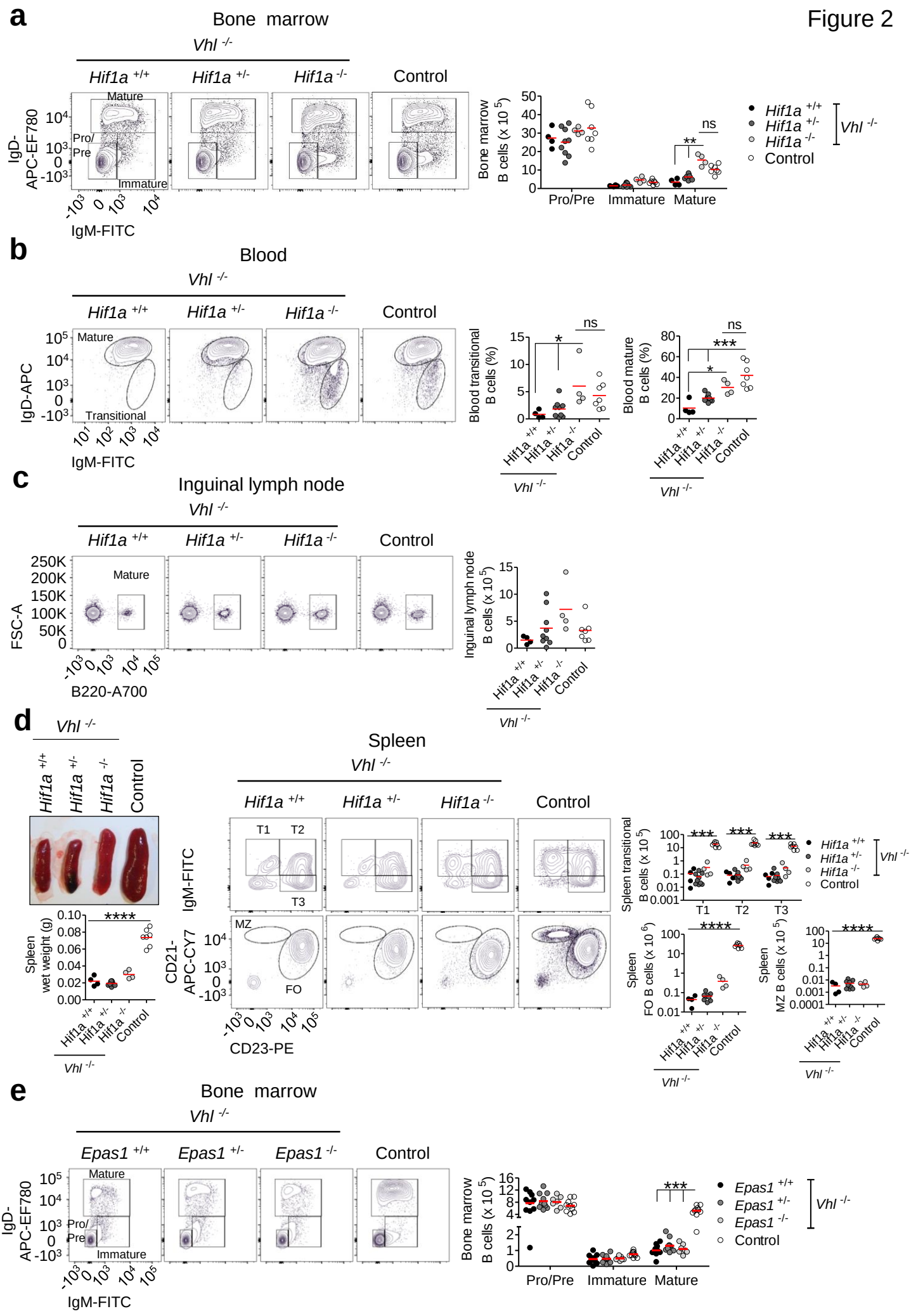
a
Bone marrow
Vhl -/-
Hif1a +/+
Hif1a +/-
Hif1a -/-
Control
Mature
Pro/
Pre
Immature
IgD-
APC-EF780
IgM-FITC
Bone marrow
B cells (x 10 5)
Pro/Pre
Immature
Mature
ns
**
Hif1a +/+
Hif1a +/-
Hif1a -/-
Control
Vhl -/-
b
Blood
Vhl -/-
Hif1a +/+
Hif1a +/-
Hif1a -/-
Control
Mature
Transitional
IgD-APC
IgM-FITC
Blood transitional
B cells (%)
Blood mature
B cells (%)
ns
*
***
Hif1a +/+
Hif1a +/-
Hif1a -/-
Control
Vhl -/-
c
Inguinal lymph node
Vhl -/-
Hif1a +/+
Hif1a +/-
Hif1a -/-
Control
Mature
FSC-A
B220-A700
Inguinal lymph node
B cells (x 10 5)
Hif1a +/+
Hif1a +/-
Hif1a -/-
Control
Vhl -/-
d
Vhl -/-
Hif1a +/+
Hif1a +/-
Hif1a -/-
Control
Spleen
Vhl -/-
Hif1a +/+
Hif1a +/-
Hif1a -/-
Control
T1
T2
T3
MZ
FO
IgM-FITC
CD21-
APC-CY7
CD23-PE
Spleen
wet weight (g)
****
Spleen transitional
B cells (x 10 5)
***
Spleen
FO B cells (x 10 6)
Spleen
MZ B cells (x 10 5)
Hif1a +/+
Hif1a +/-
Hif1a -/-
Control
Vhl -/-
e
Bone marrow
Vhl -/-
Epas1 +/+
Epas1 +/-
Epas1 -/-
Control
Mature
Pro/
Pre
Immature
IgD-
APC-EF780
IgM-FITC
Bone marrow
B cells (x 10 5)
Pro/Pre
Immature
Mature
***
Epas1 +/+
Epas1 +/-
Epas1 -/-
Control
Vhl -/-

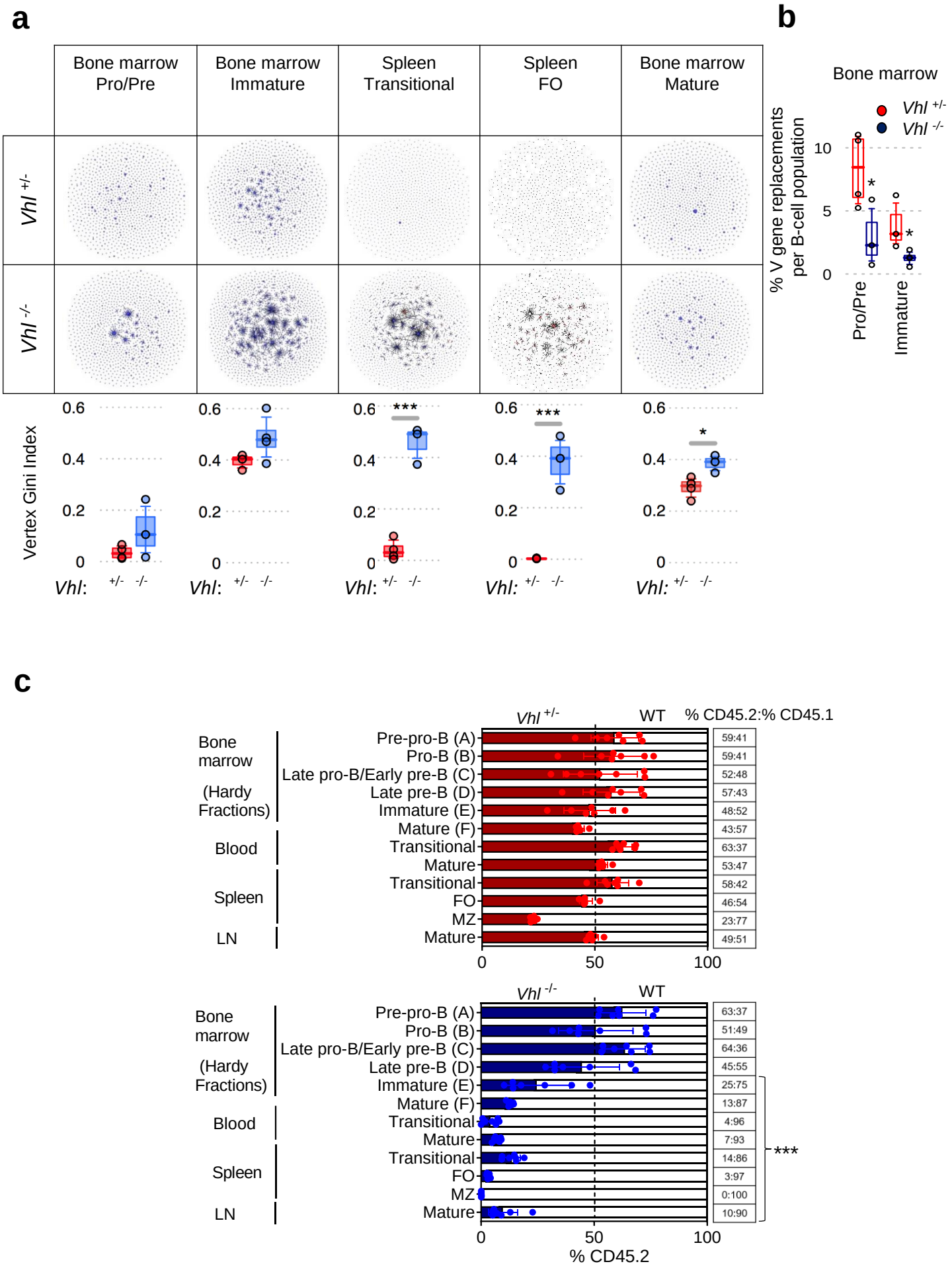
a
Bone marrow Pro/Pre
Bone marrow Immature
Spleen Transitional
Spleen FO
Bone marrow Mature
Vhl +/-
Vhl -/-
Vertex Gini Index
0.6
0.4
0.2
0
***
*
Vhl: +/- -/-
b
Bone marrow
Vhl +/-
Vhl -/-
% V gene replacements per B-cell population
10
5
0
*
Pro/Pre
Immature
c
Vhl +/-
WT
% CD45.2:% CD45.1
Bone marrow (Hardy Fractions)
Blood
Spleen
LN
Pre-pro-B (A)
Pro-B (B)
Late pro-B/Early pre-B (C)
Late pre-B (D)
Immature (E)
Mature (F)
Transitional
Mature
Transitional
FO
MZ
Mature
59:41
59:41
52:48
57:43
48:52
43:57
63:37
53:47
58:42
46:54
23:77
49:51
0
50
100
Vhl -/-
WT
63:37
51:49
64:36
45:55
25:75
13:87
4:96
7:93
14:86
3:97
0:100
10:90
***
% CD45.2

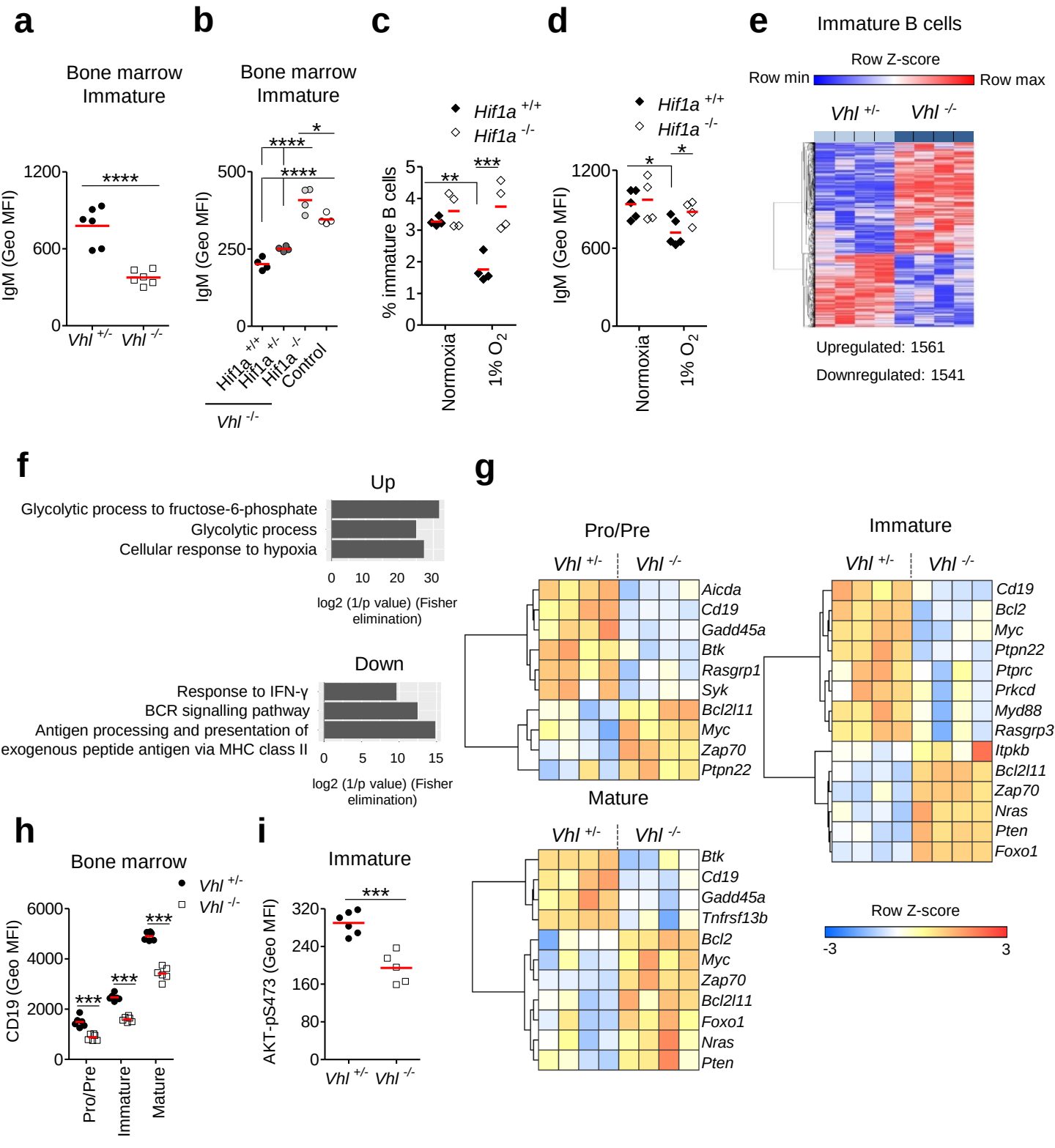
a
Bone marrow
Immature
IgM (Geo MFI)
1200
600
0
****
Vhl +/-
Vhl -/-
b
Bone marrow
Immature
IgM (Geo MFI)
500
250
0
*
****
****
Hif1a +/+
Hif1a +/-
Hif1a -/-
Control
Vhl -/-
c
Hif1a +/+
Hif1a -/-
% immature B cells
5
4
3
2
1
0
**
***
Normoxia
1% O2
d
Hif1a +/+
Hif1a -/-
IgM (Geo MFI)
1200
600
0
*
*
Normoxia
1% O2
e
Immature B cells
Row Z-score
Row min
Row max
Vhl +/-
Vhl -/-
Upregulated: 1561
Downregulated: 1541
f
Up
Glycolytic process to fructose-6-phosphate
Glycolytic process
Cellular response to hypoxia
0 10 20 30
log2 (1/p value) (Fisher elimination)
Down
Response to IFN-γ
BCR signalling pathway
Antigen processing and presentation of exogenous peptide antigen via MHC class II
0 5 10 15
log2 (1/p value) (Fisher elimination)
g
Pro/Pre
Vhl +/-
Vhl -/-
Aicda
Cd19
Gadd45a
Btk
Rasgrp1
Syk
Bcl2l11
Myc
Zap70
Ptpn22
Immature
Vhl +/-
Vhl -/-
Cd19
Bcl2
Myc
Ptpn22
Ptprc
Prkcd
Myd88
Rasgrp3
Itpkb
Bcl2l11
Zap70
Nras
Pten
Foxo1
Mature
Vhl +/-
Vhl -/-
Btk
Cd19
Gadd45a
Tnfrsf13b
Bcl2
Myc
Zap70
Bcl2l11
Foxo1
Nras
Pten
Row Z-score
-3
3
h
Bone marrow
Vhl +/-
Vhl -/-
CD19 (Geo MFI)
6000
4000
2000
0
***
***
***
Pro/Pre
Immature
Mature
i
Immature
AKT-pS473 (Geo MFI)
320
240
160
80
0
***
Vhl +/-
Vhl -/-

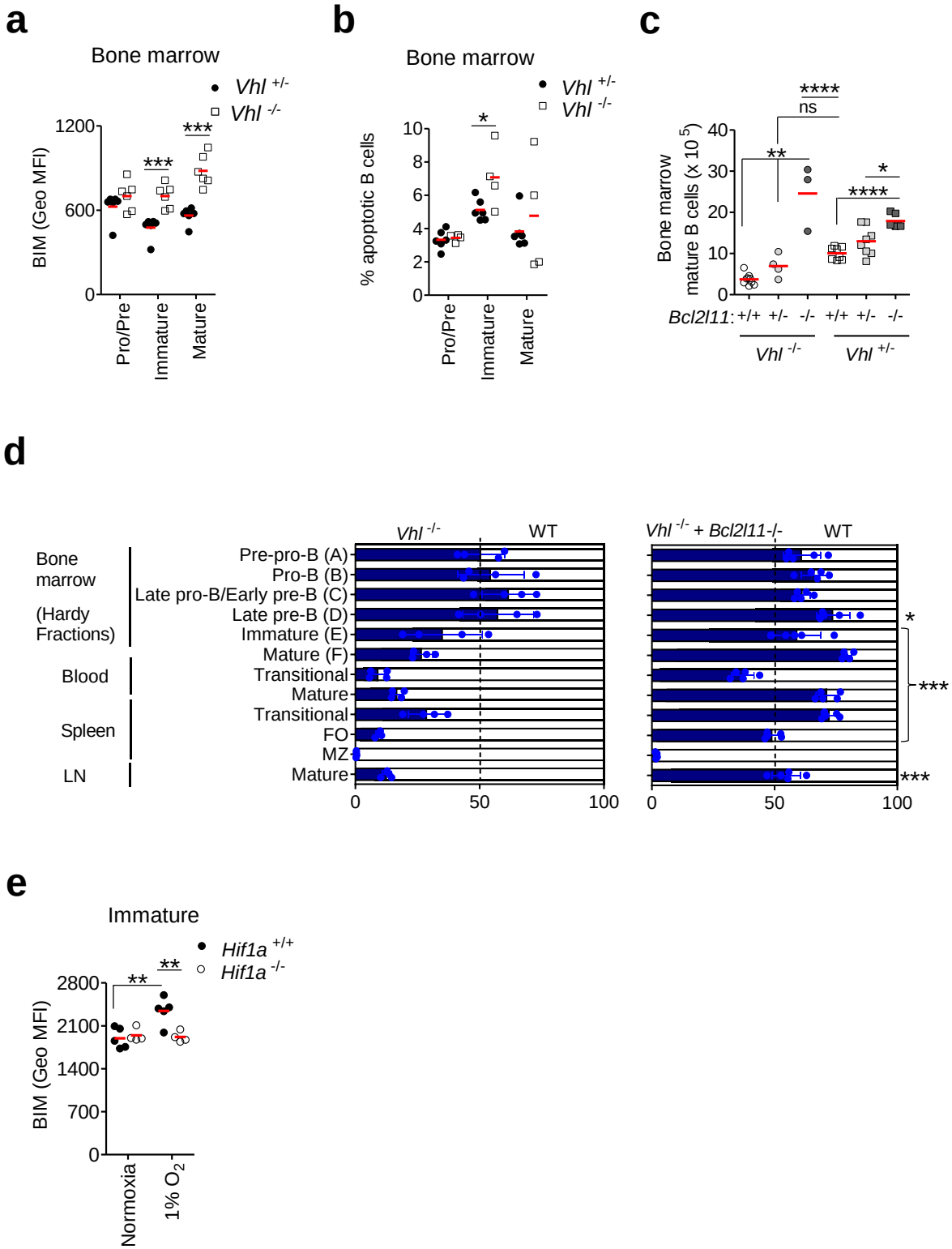
a
Bone marrow
Vhl +/-
Vhl -/-
BIM (Geo MFI)
1200
600
0
***
***
Pro/Pre
Immature
Mature
b
Bone marrow
Vhl +/-
Vhl -/-
% apoptotic B cells
10
8
6
4
2
0
*
Pro/Pre
Immature
Mature
c
Bone marrow mature B cells (x 10^5)
40
30
20
10
0
****
ns
**
*
****
Bcl2l11: +/+ +/- -/- +/+ +/- -/-
Vhl -/-
Vhl +/-
d
Vhl -/-
WT
Vhl -/- + Bcl2l11-/-
WT
Bone marrow
(Hardy Fractions)
Blood
Spleen
LN
Pre-pro-B (A)
Pro-B (B)
Late pro-B/Early pre-B (C)
Late pre-B (D)
Immature (E)
Mature (F)
Transitional
Mature
Transitional
FO
MZ
Mature
0
50
100
*
***
***
e
Immature
Hif1a +/+
Hif1a -/-
BIM (Geo MFI)
2800
2100
1400
700
0
**
**
Normoxia
1% O2

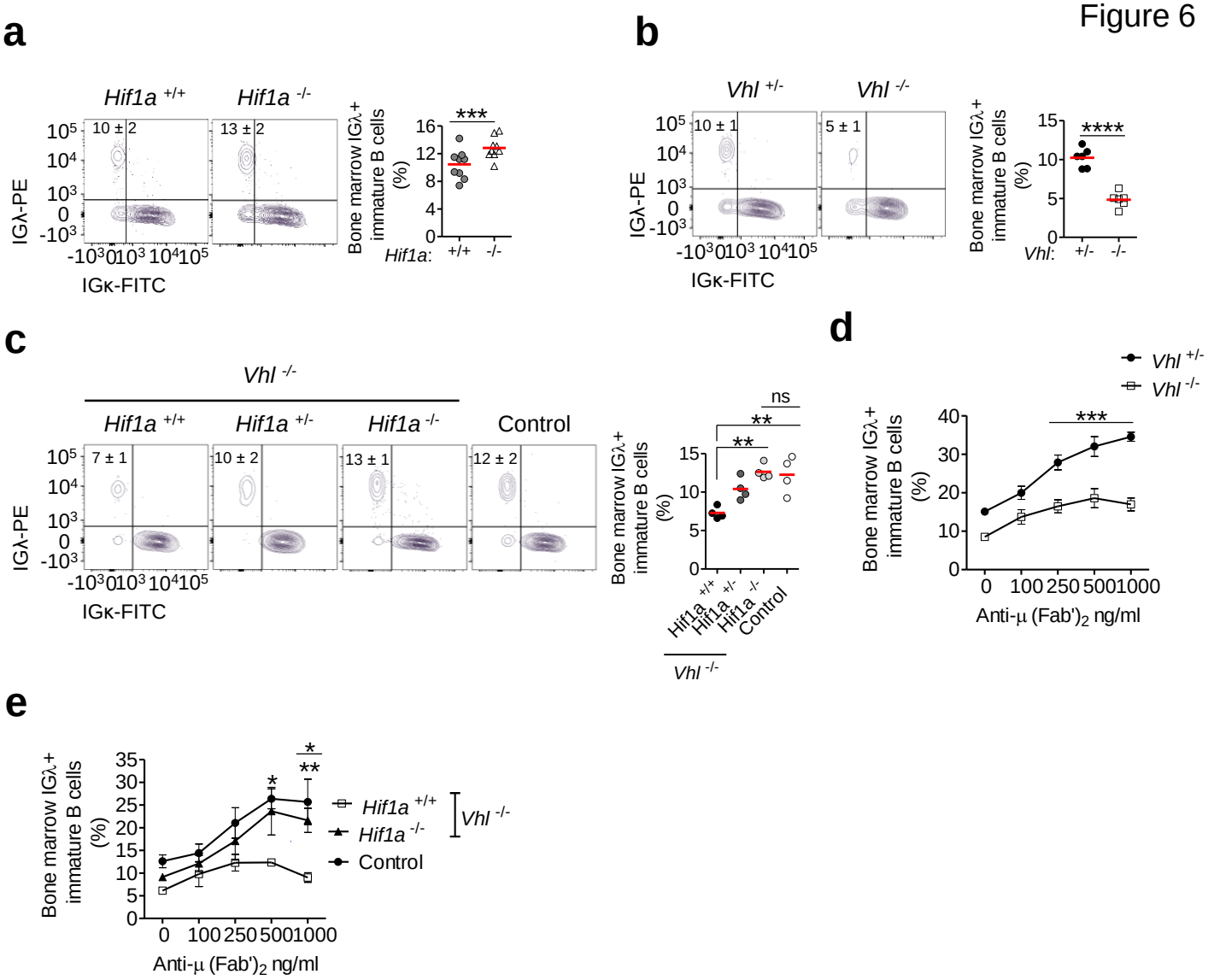
a
Hif1a +/+
Hif1a -/-
10 ± 2
13 ± 2
IGλ-PE
IGκ-FITC
Bone marrow IGλ+ immature B cells (%)
***
Hif1a: +/+ -/-
b
Vhl +/-
Vhl -/-
10 ± 1
5 ± 1
****
Vhl: +/- -/-
c
Vhl -/-
Hif1a +/+
Hif1a +/-
Hif1a -/-
Control
7 ± 1
10 ± 2
13 ± 1
12 ± 2
ns
**
**
Hif1a +/+
Hif1a +/-
Hif1a -/-
Control
Vhl -/-
d
Vhl +/-
Vhl -/-
***
Anti-μ (Fab')2 ng/ml
e
*
**
*
Hif1a +/+
Hif1a -/-
Control
Vhl -/-
Anti-μ (Fab')2 ng/ml

Figure 7

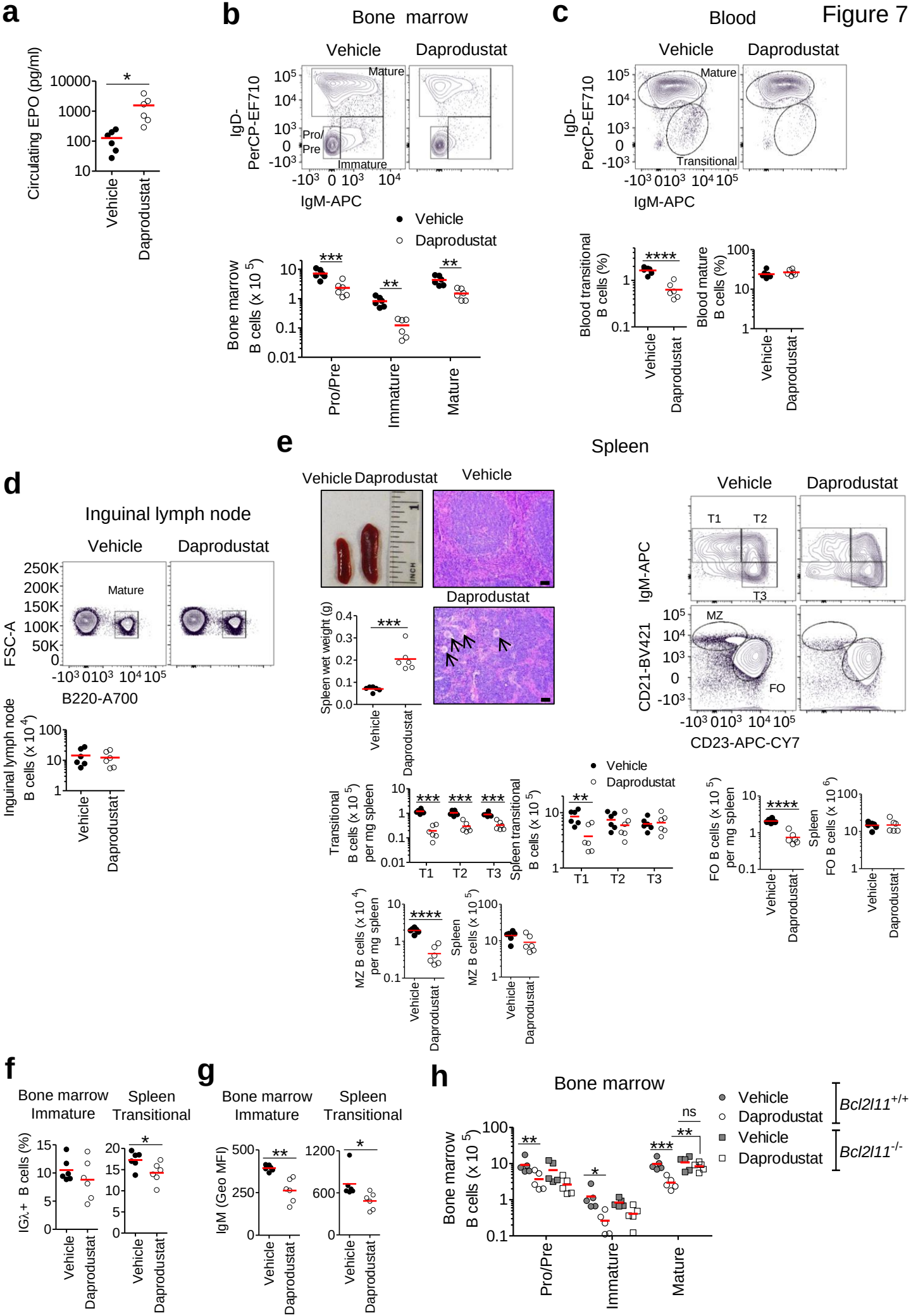
a
Circulating EPO (pg/ml)
Vehicle
Daprodustat
b
Bone marrow
Vehicle
Daprodustat
IgD-PerCP-EF710
IgM-APC
Mature
Pro/Pre
Immature
Bone marrow B cells (x 10 5)
Pro/Pre
Immature
Mature
c
Blood
Transitional
Blood transitional B cells (%)
Blood mature B cells (%)
d
Inguinal lymph node
FSC-A
B220-A700
Inguinal lymph node B cells (x 10 4)
e
Spleen
Spleen wet weight (g)
IgM-APC
CD21-BV421
CD23-APC-CY7
MZ
FO
Transitional B cells (x 10 5) per mg spleen
Spleen transitional B cells (x 10 5)
FO B cells (x 10 5) per mg spleen
Spleen FO B cells (x 10 6)
MZ B cells (x 10 4) per mg spleen
Spleen MZ B cells (x 10 5)
f
Bone marrow Immature
Spleen Transitional
IGλ+ B cells (%)
g
IgM (Geo MFI)
h
Bone marrow
Bone marrow B cells (x 10 5)
Bcl2l11+/+
Bcl2l11-/-
ns